Theory of coupled spin-charge transport due to spin-orbit interaction in inhomogeneous two-dimensional electron liquids

Ka Shen,[1] R. Raimondi,[2] and G. Vignale[1,3]

[1]*Department of Physics and Astronomy, University of Missouri, Columbia, Missouri 65211, USA*
[2]*CNISM and Dipartimento di Matematica e Fisica, Università Roma Tre, Via della Vasca Navale 84, 00146 Rome, Italy*
[3]*Donostia International Physics Center (DIPC), Manuel de Lardizabal 4, E-20018 San Sebastián, Spain*

Spin-orbit interactions in two-dimensional electron liquids are responsible for many interesting transport phenomena in which particle currents are converted to spin polarizations and spin currents and vice versa. Prime examples are the spin Hall effect, the Edelstein effect, and their inverses. By similar mechanisms, it is also possible to partially convert an optically induced electron-hole density wave to a spin density wave and vice versa. In this paper, we present a unified theoretical treatment of these effects based on quantum kinetic equations that include not only the intrinsic spin-orbit coupling from the band structure of the host material, but also the spin-orbit coupling due to an external electric field and a random impurity potential. The drift-diffusion equations we derive in the diffusive regime are applicable to a broad variety of experimental situations, both homogeneous and nonhomogeneous, and include on equal footing "skew scattering" and "side jump" from electron-impurity collisions. As a demonstration of the strength and usefulness of the theory we apply it to the study of several effects of current experimental interest: the inverse Edelstein effect, the spin-current swapping effect, and the partial conversion of an electron-hole density wave to a spin density wave in a two-dimensional electron gas with Rashba and Dresselhaus spin-orbit couplings, subject to an electric field.

I. INTRODUCTION

During the past decade, spin-orbit interactions in electron liquids have emerged as one of the most exciting topics in spintronics [1–4]. While classic spintronic devices (e.g., GMR read heads) rely on strong exchange interactions between spin-polarized conduction electrons and the local magnetization of a ferromagnetic host, spin-orbit interactions offer the possibility to couple spin and charge degrees of freedom directly in a nonmagnetic material. Outstanding examples of spin-orbital effects are the conversion of a regular electronic current into a spin current (spin Hall effect) [5–9] and the generation of a nonequilibrium spin polarization by an electronic current (Edelstein effect) [10–17]. The reciprocal effects, i.e., spin current to current [18,19] and spin polarization to current conversions [20,21], have also been observed—the latter being also known as spin galvanic effect [21–23]. These are potentially useful effects, which have already been successfully employed to generate spin currents [24], excite and detect spin waves [25,26], and apply spin-transfer torques that can reverse the orientation of the spin polarization in memory devices [27,28]. More subtle effects, such as the direct coupling of spin currents leading to "spin-current swapping" (see Sec. V C) have also been predicted [29,30] and await experimental verification. In addition, recent developments in transient spin grating spectroscopy [31–33] have opened the way to detailed studies of the coupled dynamics of spin and charge in inhomogeneous electronic structures. For example, the diffusion of a spin density wave [32] and its drift under the action of an electric field have been studied in detail [33], revealing interesting many-body effects; the existence of long-lived spin-helical states in GaAs quantum wells has been confirmed [32,34]. In a recent paper, building on a previous suggestion by Anderson *et al.* [35], we have

proposed that an electron-hole density wave in a GaAs quantum well can be partially converted into a spin density wave by the application of a strong electric field parallel to the wave fronts [36]. This and similar effects are by no means confined to conventional electron layers in GaAs: intermetallic interfaces, layered oxides, monolayer materials like MoS_2, and "functionalized graphene" [37,38] are all promising platforms for the observation of spin-charge conversion due to strong spin-orbit interaction. It is therefore important to develop a broadly applicable, easy-to-use formalism for describing the coupled evolutions of spin and charge densities and their associated currents in the presence of an external electric field. As distinct phenomena have been discussed separately by different approaches in the literature, the theoretical challenge is to provide a unified treatment of the various effects, including spin precession due to intrinsic spin-orbit coupling from the band structure of the host material, spin relaxation, spin-orbit interaction with impurities (leading to effects such as skew scattering and side jump), and spin-orbit interaction with the external electric field. Achieving such a unification will be helpful in revealing internal connections between apparently different effects and is therefore one of the main goals of our present work.

An elegant and intuitively appealing set of spin-charge coupled drift-diffusion equations, involving charge density N, the spin density $\mathbf{S}$, the charge current $\mathbf{J}$, and the spin current $\mathbf{J}^a$, was derived in Refs. [39–42] from a SU(2) gauge-field theoretical description of the spin-orbit coupling. In this paper, we rederive and extend those equations from a microscopic calculation, which allows us to capture all the relevant phenomena on spin-spin and spin-charge coupled dynamics in homogeneous and in (spin) density-modulated systems, as well as the spin current swapping effect. The

developed equations are summarized in the form

$$\partial_t N = -\partial_i J_i, \tag{1}$$

$$\partial_t S^a = -[\nabla_i J_i]^a - \delta S^a / \tau_{EY}, \tag{2}$$

$$J_i = -(v_i + D\partial_i)N - \gamma_{ij}^a J_j^a, \tag{3}$$

$$J_i^a = -v_i S^a - D[\nabla_i S]^a - \gamma_{ij}^a J_j + \kappa \left(J_a^i - \delta_{ai} J_l^l \right), \tag{4}$$

where

$$[\nabla_i V]^a \equiv \partial_i V^a - 2\epsilon^{abc} A_i^b V^c \tag{5}$$

is the SU(2)-covariant derivative of a generic vector field V^a and $\delta \mathbf{S} = \mathbf{S} - \mathbf{S}_{eq}$ is the deviation of the spin density from its equilibrium value, $\mathbf{S}_{eq}$ (thus the theory is applicable to ferromagnetic states). The upper index a labels components in spin space, while the lower index i labels components in coordinate space. The SU(2)-vector potential A_i^b describes the coupling between the bth component of the spin and the ith component of the orbital motion. In the above equations, D is the diffusion constant ($D = v_F^2 \tau / d$, where v_F is the Fermi velocity and τ the current relaxation time in d dimensions), v_i is the ith component of the macroscopic drift velocity caused by an electric field $\mathbf{E}$ ($v_i = e\tau E_i / m$), and τ_{EY} is the Elliott-Yafet (EY) spin-relaxation time [43,44]. γ_{ij}^a stands for the spin Hall tensor, which connects the J_i^a component of the spin current to the J_j component of the charge current. Its explicit form is $\gamma_{ij}^a = \theta_{SH} \epsilon^{ija}$ (Ref. [41]) where θ_{SH} known as the "spin Hall angle": this is a direct manifestation of the SU(2) magnetic field, i.e., the covariant curl of the SU(2) vector potential. κ is the spin-current swapping constant, derived in Appendix D. Lastly, ϵ^{abc} is the Levi-Civita antisymmetric tensor, and a sum over repeated indices is implied throughout.

Equations (1)–(4) have a transparent physical meaning. For example, the second equation is the generalized continuity equation for the spin density. The relaxation term $-\delta S^a / \tau_{EY}$ takes into account the EY spin-relaxation process resulting from the spin-orbit interaction with impurities. At the same time, the spin precession that occurs between electron-impurity collisions and is responsible for the D'yakonov-Perel' (DP) spin-relaxation mechanism [45] is taken into account by the vector potential term in the SU(2)-covariant derivative. The last two equations have a similarly transparent meaning: they express the current (spin current) as a sum of drift, diffusion, and inverse (direct) spin Hall currents. In particular, as we will show below, it is the diffusion part of the spin current that yields the DP spin relaxation once is inserted back into the continuity equation for the spin density. Additional source terms, such as spin injection and spin electric fields can be added to the right-hand sides of these equations [40,46]. For example, a Zeeman field $\mathbf{H}$ coupling to the spin density enters the spin continuity equation through an additional precessional term $\propto (\mathbf{H} \times \mathbf{S})^a$ on the right-hand side of Eq. (2), and an additional spin current driving term $\sigma_s (\nabla_i H)^a$ on the right-hand side of Eq. (4), where σ_s is the homogeneous spin-current conductivity. At the same time, the equilibrium spin density $\mathbf{S}_{eq}$ must be reinterpreted as the quasiequilibrium spin density in the presence of the instantaneous (frozen) field $\mathbf{H}(t)$.

The application of Eqs. (1)–(4) to homogeneous spin-orbit coupled systems has demonstrable advantages over more microscopic approaches, such as nonequilibrium Green's function theory and quantum kinetic equations. The quantities considered here—densities and their associated currents—are all obtained as integrals of the nonequilibrium Green's function over frequency and momenta. While the integrated quantities contain less information than the underlying Green's function, they are more directly connected to the experimental description of the phenomena. Furthermore, there are certain features of the exact kinetics that are "hard-wired" in the macroscopic drift-diffusion equations, whereas in the microscopic theory, they only emerge from a careful enumeration of diagrams and delicate cancellations of seemingly different terms. For example, the infamous "nonanalyticity puzzle," whereby the spin Hall conductivity of the Rashba model appears to drop suddenly from a finite value to zero as soon as the Rashba spin-orbit coupling is turned on, is completely demystified: the EY relaxation time—a quantity of second order in the strength of the extrinsic spin-orbit coupling—provides the energy scale against which the Rashba spin-orbit coupling must be assessed as large or small [42]. In a more recent application, the simple addition of a spin injection term to the right-hand side of Eq. (2) has enabled us to successfully analyze the inverse Edelstein effect (also known as spin-galvanic effect), i.e., the generation of charge current from a nonequilibrium spin accumulation [20–23]. The SU(2) theory is also easily applicable to spin-charge conversion phenomena that occur in *inhomogeneous* systems. We have in mind, in particular, the electron-hole density waves and the spin density waves that can be generated by letting two noncollinear laser beams with different polarization interfere with each other on the surface of a semiconductor quantum well [31,32]. Recent experiments have demonstrated that it is possible to probe in real time (on a picosecond time scale) not only the diffusive dynamics of these inhomogeneous structures, but also their drift under the action of an externally imposed electric field [33,47]. The (spin) Hall transport dynamics is also in principle accessible to these experimental techniques. Experience with homogeneous transport phenomena suggests that an extended SU(2) formulation would be a very useful theoretical tool for the description of inhomogeneous systems. This paper presents such a formulation.

In comparison with previous derivations of spin-charge coupled drift-diffusion equations for two-dimensional electronic systems [35,48–52], the present formulation is characterized by a careful inclusion of the spin-orbit interaction between the electrons and the impurities, as well as the external electric field. To this end, we have carefully re-derived the kinetic equation in inhomogeneous systems, taking into account the spin-orbit coupling with the impurities and the electric field to the leading order that allows us to capture effects such as "side jump and "spin-current swapping," which were not included in our previous studies of inhomogeneous density/spin dynamics [36].

At last, all the relevant terms are included in the form of a generalized drift-diffusion equation. It is found that the couplings between the spin and charge components are simply

characterized by a single parameter (spin Hall angle) and, quite satisfactorily, skew scattering, side jump, and intrinsic contributions enter the spin Hall angle on equal terms, i.e., additively. On the other hand, the full spin Hall conductivity cannot be simply expressed as the sum of intrinsic and extrinsic contributions for reasons that have already been discussed in the literature [42,53] and will be further explained below. Moreover, we predict that only the diffusion-induced spin current can produce a swapping effect. The resulting equations for spin and charge densities and their currents provide a unified theoretical framework within which one can easily treat both homogeneous and nonhomogeneous spin-charge conversion phenomena, such as the spin Hall effect, the Edelstein effect, the spin-current swapping effect, and the partial conversion of an electron-hole density wave into a spin density wave under the application of an electric field parallel to the wave fronts. Throughout the paper we will emphasize the main concepts and present the final results of complex calculations. The interested reader will find the details of the derivations in the appendices. We point out that Eqs. (1)–(4) are valid for a broad class of intrinsic spin-orbit couplings that are linear in momentum. Different forms of the spin-orbit coupling may require modifications, which, however, can still be derived from the kinetic equation approach described in this paper.

II. MODEL HAMILTONIAN

The theory we are going to present applies to two-dimensional model Hamiltonians of the form

$$H = H_{\text{eff}}(\hat{\mathbf{p}}) + H_E(\mathbf{r}) + H_V(\mathbf{r}), \tag{6}$$

where

$$H_{\text{eff}}(\hat{\mathbf{p}}) = \frac{\hat{\mathbf{p}}^2}{2m} + \frac{1}{m} \sum_{i,j} \hat{p}_i A_i^j \sigma^j \tag{7}$$

is an effective mass Hamiltonian for electrons with momentum operator $\hat{\mathbf{p}} = -i\nabla_{\mathbf{r}}$, σ^j are Pauli matrices for the spin and A_i^j are the components of a uniform spin-dependent [SU(2)] vector potential, which describes both the effective spin-orbit interaction with the crystal lattice and the spin-orbit interaction with an in-plane field $\mathbf{E}$. In addition, we have two terms that break the conservation of crystal momentum:

$$H_E(\mathbf{r}) = e\mathbf{E} \cdot \mathbf{r}, \tag{8}$$

is the regular interaction with an in-plane uniform electric field $\mathbf{E}$, and

$$H_V(\mathbf{r}) = V(\mathbf{r}) - \alpha'\boldsymbol{\sigma} \times \nabla_{\mathbf{r}}V(\mathbf{r}) \cdot \hat{\mathbf{p}}, \tag{9}$$

is the complete electron-impurity potential, of which $V(\mathbf{r})$ is the spin-independent part and $\alpha'\boldsymbol{\sigma} \times \nabla_{\mathbf{r}}V(\mathbf{r}) \cdot \hat{\mathbf{p}}$ the spin-orbit coupling part (only nonmagnetic impurities are considered). Here, $\alpha' \equiv \lambda_c^2/4$ is the square of the effective Compton wavelength for the material under study ($\alpha' \sim 5$ Å^2 in GaAs). The presence of the spin-orbit term in Eq. (9) is essential for the extrinsic spin Hall effect.

As a concrete example, consider the case of a (001) quantum well in a semiconductor of the zinc-blende structure (e.g., GaAs) with Rashba and Dresselhaus interactions and an in-plane electric field $\mathbf{E}$. Then the nonvanishing components of the SU(2) vector potential are

$$A_x^y = m\lambda_1, \quad A_y^x = m\lambda_2,$$
$$A_x^z = m\alpha'eE_y, \quad A_y^z = -m\alpha'eE_x, \tag{10}$$

where $\lambda_1 = \alpha + \beta$ and $\lambda_2 = \beta - \alpha$ with α and β being the Rashba [54] and Dresselhaus [55] SOC coefficients separately. Following common usage, the x and y axes are defined in the [110] and [$\bar{1}$10] directions, respectively. The two terms on the last line describe the spin-orbit interaction with the in-plane electric field.

For future use, we also define, in momentum space, the crystal and electric-field-induced spin-orbit coupling energy, $H_{\mathbf{k}}^{\text{soc}}$, for the electron state with momentum $\mathbf{k}$, as follows:

$$H_{\mathbf{k}}^{\text{soc}} \equiv \frac{1}{m} \sum_{ij} k_i A_i^j \sigma^j, \tag{11}$$

such that the total energy from H_{eff} reads

$$H_{\mathbf{k}} = \varepsilon_k + H_{\mathbf{k}}^{\text{soc}}, \tag{12}$$

where $\varepsilon_k = \frac{k^2}{2m}$.

III. KINETIC EQUATION

Our starting point is the well-known [4,56] kinetic equation for the quasiclassical (Wigner) distribution function $\rho_{\mathbf{k}}(\mathbf{r},t)$:

$$\partial_t\rho_{\mathbf{k}} + i[H_{\mathbf{k}},\rho_{\mathbf{k}}] + \tfrac{1}{2}\{\nabla_{\mathbf{k}}H_{\mathbf{k}},\nabla_{\mathbf{r}}\rho_{\mathbf{k}}\} - e\mathbf{E} \cdot \nabla_{\mathbf{k}}\rho_{\mathbf{k}} = I_{\mathbf{k}}. \tag{13}$$

All the quantities in this equation, including the collision integral $I_{\mathbf{k}}$, are functions of a position $\mathbf{r}$ and a time t, which are not explicitly written down. Here, the symbols [,] and { ,} stand for commutator and anticommutator, respectively and all quantities are matrices in spin space. The collision integral $I_{\mathbf{k}}$ arises from the interaction with impurities, Eq. (9), and is expressed in terms of the contour-ordered Green's function $G_{\mathbf{k}}(\mathbf{r},t,t')$ and the self-energy $\Sigma_{\mathbf{k}}(\mathbf{r},t,t')$ as

$$I_{\mathbf{k}}(t) = - \left(\int_c dt'[\Sigma_{\mathbf{k}}(t,t')G_{\mathbf{k}}(t',t) - G_{\mathbf{k}}(t,t')\Sigma_{\mathbf{k}}(t',t)] \right)^<, \tag{14}$$

where the superscript $<$ denotes the lesser component of the contour integral. Details of the derivation can be found in Refs. [57] and [58].

The self-energy due to the impurity potential consists of four terms, which are graphically represented in Fig. 1. For a short-range δ-correlated disorder potential $V(\mathbf{r}) = \sum_i v_0\delta(\mathbf{r} - \mathbf{R}_i)$, where $\mathbf{R}_i$ are the random position of impurities with average density n_i, these diagrams have the following
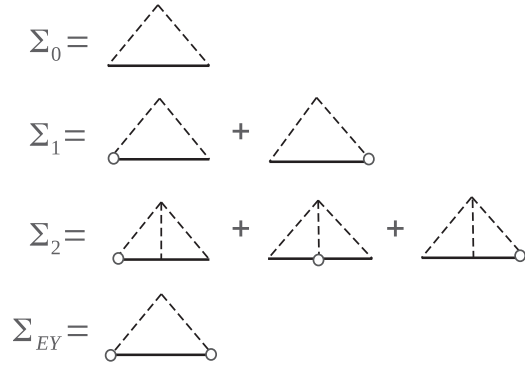
FIG. 1. Diagrams for the impurity-averaged self-energy Σ_0, Σ_1, Σ_2, and Σ_{EY}. The dashed line denotes the impurity averge and the vertices with open circles represent the impurity-induced spin-orbit coupling.

analytic expressions (see Refs. [39] and [42]):

$$\Sigma_{0\mathbf{k}} = n_i v_0^2 \sum_{\mathbf{k}'} G_{\mathbf{k}'}\,, \tag{15}$$

(i.e., the usual Born approximation)

$$\Sigma_{1\mathbf{k}} = n_i v_0^2 \alpha' \sum_{\mathbf{k}'} \left(-i[\boldsymbol{\sigma} \cdot \mathbf{k} \times \mathbf{k}', G_{\mathbf{k}'}] \right.$$
$$\left. -\frac{1}{2}\{\boldsymbol{\sigma} \times (\mathbf{k} - \mathbf{k}'), \nabla_{\mathbf{r}} G_{\mathbf{k}'}\} \right), \tag{16}$$

and

$$\Sigma_{2\mathbf{k}} = -i n_i v_0^3 \alpha' \sum_{\mathbf{k}',\mathbf{k}''} (\mathbf{k} \times \mathbf{k}' \cdot \boldsymbol{\sigma}\, G_{\mathbf{k}'} G_{\mathbf{k}''}$$
$$+ G_{\mathbf{k}'} \mathbf{k}' \times \mathbf{k}'' \cdot \boldsymbol{\sigma}\, G_{\mathbf{k}''} + G_{\mathbf{k}'} G_{\mathbf{k}''} \mathbf{k}'' \times \mathbf{k} \cdot \boldsymbol{\sigma}). \tag{17}$$

The gradient term in $\Sigma_{1\mathbf{k}}$ comes from the derivative operator in Eq. (9) acting on the spatial argument of the Green function. A similar gradient term in $\Sigma_{2\mathbf{k}}$ is neglected on account of its smallness in a system with smooth inhomogeneity. The last diagram, denoted by Σ_{EY} is given by [39]

$$\Sigma_{EY\mathbf{k}} = n_i v_0^2 (\alpha')^2 \sum_{\mathbf{k}'} \sigma^z G_{\mathbf{k}'} \sigma^z (\mathbf{k} \times \mathbf{k}')_z^2 \tag{18}$$

and is responsible for Elliott-Yafet spin relaxation.

To write out the collision integral in terms of the density matrix $\rho_{\mathbf{k}}$, we employ the standard rules of analytic continuation [57] combined with the generalized Kadanoff-Baym ansatz [57,59], which expresses the lesser or greater components of the Green's function (and hence the self-energy) in terms of equal-time Green's functions and retarded/advanced

propagators:[1]

$$G_{\mathbf{k}}^{\gtrless}(\mathbf{r},t,t_1) = \mp i[\theta(t - t_1) e^{-i\tilde{H}(t-t_1)} \rho_{\mathbf{k}}^{\gtrless}(\mathbf{r},t_1)$$
$$+ \theta(t_1 - t) \rho_{\mathbf{k}}^{\gtrless}(\mathbf{r},t) e^{-i\tilde{H}(t-t_1)}]. \tag{19}$$

Here, $\rho_{\mathbf{k}}^< = \rho_{\mathbf{k}}$ and $\rho_{\mathbf{k}}^> = 1 - \rho_{\mathbf{k}}$. Notice that the Hamiltonian $\tilde{H}$ contains not only $H_{\mathbf{k}}$, but also the electric potential H_E, i.e., $\tilde{H}(\mathbf{r},\mathbf{k}) = H_{\mathbf{k}} + H_E(\mathbf{r})$. According to Refs. [60] and [61], the inclusion of H_E is essential to capture the full side-jump effect.

Treating the SOCs and electric potential as small perturbations,[2] we expand the propagator in Eq. (19) as [60,61]

$$e^{-i\tilde{H}\tilde{t}} \approx e^{-i\varepsilon_k \tilde{t}} \left(1 - i\tilde{t} H_{\mathbf{k}}^{\text{soc}} - i\tilde{t} H_E\right), \tag{20}$$

where $\tilde{t} \equiv t - t_1$. To construct the collision integral, we separately consider the contributions arising from the first, the second, and the third term in the brackets in Eq. (20).

A. Collision integral from unperturbed propagator

The first term in the brackets in Eq. (20), when substituted in Eq. (19) and subsequently in the expression (14) for the collision integral leads to

$$I_{\mathbf{k}}^{(0)} = n_i v_0^2 \sum_{\mathbf{k}'} 2\pi \delta(\varepsilon_k - \varepsilon_{k'}) \left[(\rho_{\mathbf{k}'} - \rho_{\mathbf{k}}) \right.$$
$$\left. - i\alpha'[\boldsymbol{\sigma} \cdot \mathbf{k} \times \mathbf{k}', \rho_{\mathbf{k}'}] - \frac{1}{2}\{\alpha'\boldsymbol{\sigma} \times (\mathbf{k} - \mathbf{k}'), \partial_{\mathbf{r}} \rho_{\mathbf{k}'}\} \right] \tag{21}$$

(from Σ_0 and Σ_1). Here the first term, proportional to $(\rho_{\mathbf{k}'} - \rho_{\mathbf{k}})$, arises from $\Sigma_{0\mathbf{k}}$ and describes ordinary electron-impurity scattering processes. The remaining two terms arise from the two parts of $\Sigma_{1\mathbf{k}}$ in Eq. (16) and are less familiar. The second term describes the spin precession that occurs during a single electron-impurity collision, with the precession angle depending on the relative angle between the momenta before and after collision. This spin precession, as we will show later, can manifest itself through the "spin-current swapping" [29]. The third term with the gradient of the density matrix gives rise to a spin density coupling proportional to the change in

---

[1]We have substituted the relation between equal-time Green function and nonequilibrium distribution function $G_{\mathbf{k}}^<(t,t) = i\rho_{\mathbf{k}}(t)$ and $G_{\mathbf{k}}^>(t,t) = -i[1 - \rho_{\mathbf{k}}(t)]$ and the free retarded and advanced Greens function, i.e., $G_{\mathbf{k}}^r(t,t_1) = -i\theta(t - t_1)e^{-iH_{\mathbf{k}}(t-t_1)}$ and $G_{\mathbf{k}}^a(t,t_1) = i\theta(t_1 - t)e^{-iH_{\mathbf{k}}(t-t_1)}$ into the well-known expression of the generalized Kadanoff-Baym ansatz $G_{\mathbf{k}}^{\gtrless}(t,t_1) = i[G_{\mathbf{k}}^r(t,t_1)G_{\mathbf{k}}^{\gtrless}(t_1,t_1) - G_{\mathbf{k}}^{\gtrless}(t,t)G_{\mathbf{k}}^a(t,t_1)]$. Note that we neglect the correction due to the impurity potential in $G_{\mathbf{k}}^{\gtrless}(t,t_1)$ by taking into account the fact that the leading term in the collision integral (linear order in impurity concentration) is sufficient to describe the present weak-disordered case.

[2]We assume that the electric field lies in the linear response regime and the SOC is weak, so that the spin precession angle between two collision events is much smaller than 1.

momentum. By introducing the standard relaxation time, i.e.,

$$n_i v_0^2 \sum_{\mathbf{k}'} 2\pi \delta(\varepsilon_k - \varepsilon_{k'}) = n_i m v_0^2 = \frac{1}{\tau}, \qquad (22)$$

($\hbar = 1$), we obtain

$$I_{\mathbf{k}}^{(0)} = -\frac{\rho_{\mathbf{k}} - \rho_k}{\tau} - \frac{1}{\tau} \int \frac{d\theta_{\mathbf{k}'}}{2\pi} i\alpha' [\boldsymbol{\sigma} \cdot \mathbf{k} \times \mathbf{k}', \rho_{\mathbf{k}'}]$$
$$+ \frac{1}{2} \{\alpha' \boldsymbol{\sigma} \times (\mathbf{k} - \mathbf{k}'), \partial_{\mathbf{r}} \rho_{\mathbf{k}'}\}, \qquad (23)$$

where ρ_k corresponds to the angular average of $\rho_{\mathbf{k}}$ over wave vectors of fixed magnitude $|\mathbf{k}| = k$. Similarly, the self-energy Σ_2 generates the skew-scattering contribution $I_{\mathbf{k}}^{\text{ss}}$ to the collision integral [42,62]

$$I_{\mathbf{k}}^{\text{ss}} = -n_i \alpha' \frac{m^2 v_0^3}{2} \int \frac{d\theta_{\mathbf{k}'}}{2\pi} \{\mathbf{k} \times \mathbf{k}' \cdot \boldsymbol{\sigma}, \rho_{\mathbf{k}'}\}, \qquad (24)$$

and the self-energy Σ_{EY} generates the EY spin-relaxation contribution to the collision integral:

$$I_{\mathbf{k}}^{\text{EY}} = -\frac{1}{\tau} (\alpha')^2 \int \frac{d\theta_{\mathbf{k}'}}{2\pi} (\mathbf{k} \times \mathbf{k}')_z^2 (\rho_{\mathbf{k}} - \sigma^z \rho_{\mathbf{k}'} \sigma^z). \qquad (25)$$

B. Collision integral from first-order SOC correction to the propagator

The second term in the brackets in Eq. (20), when substituted in Eq. (19) and subsequently in the expression (14) for the collision integral generates two terms related to $\Sigma_{0\mathbf{k}}$ and $\Sigma_{1\mathbf{k}}$, which we denote by $I_{\mathbf{k}}^{(a)}$ and $I_{\mathbf{k}}^{(b)}$, respectively. Their analytic expressions are

$$I_{\mathbf{k}}^{(a)} = n_i v_0^2 \sum_{\mathbf{k}'} \pi \{H_{\mathbf{k}}^{\text{soc}} - H_{\mathbf{k}'}^{\text{soc}}, \rho_{\mathbf{k}'} - \rho_{\mathbf{k}}\} \partial_{\varepsilon_k} \delta(\varepsilon_k - \varepsilon_{k'})$$
$$(26)$$

(from Σ_0) and

$$I_{\mathbf{k}}^{(b)} = n_i v_0^2 \sum_{\mathbf{k}'} \pi \Big(\{H_{\mathbf{k}}^{\text{soc}}, [(-i\alpha' \vec{\sigma} \cdot \mathbf{k} \times \mathbf{k}'), \rho_{\mathbf{k}'}]\}$$
$$+ \{\rho_{\mathbf{k}}, [(-i\alpha' \vec{\sigma} \cdot \mathbf{k} \times \mathbf{k}'), H_{\mathbf{k}'}^{\text{soc}}]\}$$
$$+ [i\alpha' \vec{\sigma} \cdot \mathbf{k} \times \mathbf{k}', \{\rho_{\mathbf{k}'}, H_{\mathbf{k}'}^{\text{soc}}\}] \Big) \partial_{\varepsilon_k} \delta(\varepsilon_k - \varepsilon_{k'}), \qquad (27)$$

(from Σ_1). We notice that $I_{\mathbf{k}}^{(a)}$ simply describes the SOC-induced shift in the single particle energies that enter the δ function of conservation of energy. In the relaxation time approximation, this term can be readily evaluated as [36]

$$I_{\mathbf{k}}^{(a)} = \frac{1}{2\tau} \{H_{\mathbf{k}}^{\text{soc}}, \partial_{\varepsilon_k} \rho_k\}. \qquad (28)$$

In contrast to this, a similar relaxation time approximation form cannot be derived for $I_{\mathbf{k}}^{(b)}$ in a simple way, because of the complicated dependence on both $\mathbf{k}$ and $\mathbf{k}'$. Fortunately, this part is already of the order that is required for the description of the side-jump effect, namely first order in band SOC together with first order in α', which allows us to extract its contribution to the drift-diffusion equation, as detailed in Appendix B. One may notice that the second and third terms in $I_{\mathbf{k}}^{(b)}$ describe the "anomalous spin precession" introduced in Ref. [61], here generalized to spin-polarized distributions.

C. Collision integral from electric field correction to the propagator

Finally, the electric potential correction to the propagator, i.e., the third term in the brackets of Eq. (20), when combined with the self-energy $\Sigma_{1\mathbf{k}}$, leads to a contribution to the collision integral of the form

$$I_{\mathbf{k}}^{(c)} = n_i v_0^2 \sum_{\mathbf{k}'} \pi \{\alpha' e\mathbf{E} \cdot \boldsymbol{\sigma} \times (\mathbf{k} - \mathbf{k}'), \rho_{\mathbf{k}'} - \rho_{\mathbf{k}}\}$$
$$\times \left[\partial_{\varepsilon_k} \delta(\varepsilon_k - \varepsilon_{k'}) \right]. \qquad (29)$$

By comparison with Eq. (26) one can see that this term equals the contribution due to electric-field-induced SOC in $I_{\mathbf{k}}^{(a)}$, reflecting the famous factor of "2" in the side jump effect [60,63,64]. In the relaxation time approximation it takes the form

$$I_{\mathbf{k}}^{(c)} = \frac{1}{2\tau} \{\alpha' e\mathbf{E} \cdot \boldsymbol{\sigma} \times \mathbf{k}, \partial_{\varepsilon_k} \rho_k\}. \qquad (30)$$

The remaining parts of the self-energy, Σ_2 and the gradient term in Σ_1, combined with the second and third terms in the brackets in Eq. (20), give higher-order contributions, which are therefore neglected.

D. Full collision integral

Our complete expression for the collision integral is therefore

$$I_{\mathbf{k}} = I_{\mathbf{k}}^{(0)} + I_{\mathbf{k}}^{(a)} + I_{\mathbf{k}}^{(b)} + I_{\mathbf{k}}^{(c)} + I_{\mathbf{k}}^{\text{ss}} + I_{\mathbf{k}}^{\text{EY}}. \qquad (31)$$

Compared to our previous calculation in Ref. [36], where the collision term was given by

$$I_{\mathbf{k}} = -\frac{\rho_{\mathbf{k}} - \rho_k}{\tau} + \frac{1}{2\tau} \{H_{\mathbf{k}}^{\text{soc}}, \partial_{\varepsilon_k} \rho_k\} + I_{\mathbf{k}}^{\text{ss}}, \qquad (32)$$

our careful treatment with impurity-induced SOC has produced several additional contributions, such as $I_{\mathbf{k}}^{(b)}$, $I_{\mathbf{k}}^{(c)}$, and $I_{\mathbf{k}}^{\text{EY}}$, as well as the second and the third terms in $I_{\mathbf{k}}^{(0)}$. Such terms describe interesting physical effects, e.g., the spin precession within a single collision due to SOC induced by impurity potential and/or band SOC. Even though some of these terms had been obtained and discussed separately for specific systems in literature [29,42,61], our derivation pulls all the pieces together while supplying a more general and complete kinetic theory for spatially inhomogeneous system.

IV. DRIFT-DIFFUSION EQUATIONS

The density matrix provides a microscopic description of transport—one in which we keep track of the detailed distribution of electrons in momentum space. Such a detailed description is often unnecessary. For example, when studying spintronic devices we are usually interested in equations that connect the spin and charge currents to the corresponding densities in space: information about the momentum distribution of the particles is discarded. We are thus facing the task of reducing the kinetic equations to more manageable equations for the charge and spin densities and current densities. Such equations are referred to as "drift-diffusion equations," and this section presents the main steps in their derivation. More

precisely, in Sec. IV A, we derive the equations that govern the evolution of the densities, without explicit reference to the currents. Explicit formulas for the currents are derived in Sec. IV B.

A. Equations for the densities

We begin by expanding the density matrix as $\rho_{\mathbf{k}} = g_{\mathbf{k}}^i \sigma^i$ and $\rho_k = g_k^i \sigma^i$. Here, in addition to the familiar Pauli matrices $\sigma^1 = \sigma_x$, $\sigma^2 = \sigma_y$, and $\sigma^3 = \sigma_z$, we have also included, for convenience, the 2×2 identity matrix $\sigma^0 = \mathbf{1}$. Thus $g_{\mathbf{k}}^0$ represents the charge distribution regardless of spin orientation. Similarly, we expand the collision integral as $I_{\mathbf{k}} = I_{\mathbf{k}}^i \sigma^i$.

After the Fourier transformation with respect to t and $\mathbf{r}$, with conjugate variables ω and $\mathbf{q}$, respectively, the kinetic equation is rewritten as

$$(\mathcal{I} + \mathcal{K}_{\mathbf{k}})\mathbf{g}_{\mathbf{k}} = (\mathcal{I} + \mathcal{T}_{\mathbf{k}})\mathbf{g}_k + \int \frac{d\theta_{\mathbf{k}'}}{2\pi} \mathcal{M}_{\mathbf{k},\mathbf{k}'}\mathbf{g}_{\mathbf{k}'} + \tau \mathbf{I}_{\mathbf{k}}^{(b)}, \quad (33)$$

where $\mathbf{g}$ is a column vector with components (g^0, g^1, g^2, g^3) and $\mathbf{I}$ is also a column vector with components (I^0, I^1, I^2, I^3). Here, $\mathcal{I}$ is the 4×4 identity matrix and $\mathcal{K}_{\mathbf{k}}$, defined in Appendix A, generates what is essentially the scattering-free dynamics of the density matrix. The right-hand side of Eq. (33) includes all the relevant collision terms derived in the previous section, with the matrices $\mathcal{T}_{\mathbf{k}}$ and $\mathcal{M}_{\mathbf{k},\mathbf{k}'}$ defined in Appendix A. Notice that, due to the spatial Fourier transformation, the matrices $\mathcal{K}_{\mathbf{k}}$, $\mathcal{T}_{\mathbf{k}}$ and $\mathcal{M}_{\mathbf{k},\mathbf{k}'}$, which were previously functions of $\mathbf{r}$, have now become functions of the conjugate wave vector $\mathbf{q}$ (see Appendix A).

In the limit in which the extrinsic SOC constant α' vanishes, the kinetic equation can be solved (by exploiting its relaxation time approximation form) yielding

$$\mathbf{g}_{\mathbf{k}}(\alpha' = 0) = [(\mathcal{I} + \mathcal{K}_{\mathbf{k}})^{-1}(\mathcal{I} + \mathcal{T}_{\mathbf{k}})]\mathbf{g}_k \equiv \tilde{\mathbf{g}}_{\mathbf{k}}. \quad (34)$$

Notice that the full angle dependence (direction of $\mathbf{k}$) of $\mathbf{g}_{\mathbf{k}}$ is entirely determined by the $\mathbf{k}$ dependence of the matrices $\mathcal{K}_{\mathbf{k}}$ and $\mathcal{T}_{\mathbf{k}}$. Hence, in this limit of vanishing extrinsic SOC, by taking the angle average over $\mathbf{k}$ in Eq. (34) one can obtain a closed equation for the angle averaged density matrix vector $\mathbf{g}_k$. In the diffusive regime, the relaxation time is very short compared to the time scale over which the distribution function varies significantly. Therefore the effect of α' is a small correction to the collision integral. Substituting $\mathbf{g}_{\mathbf{k}} \simeq \tilde{\mathbf{g}}_{\mathbf{k}}$ into the scattering terms on the right-hand side of Eq. (33)

yields

$$\mathbf{g}_{\mathbf{k}} \simeq \tilde{\mathbf{g}}_{\mathbf{k}} + (\mathcal{I} + \mathcal{K}_{\mathbf{k}})^{-1}\left[\int \frac{d\theta_{\mathbf{k}'}}{2\pi} \mathcal{M}_{\mathbf{k},\mathbf{k}'}\tilde{\mathbf{g}}_{\mathbf{k}'} + \tau I_{\mathbf{k}}^{(b)}(\tilde{\mathbf{g}}_{\mathbf{k}}, \tilde{\mathbf{g}}_{\mathbf{k}'}) \right]. \quad (35)$$

Now all terms on the right-hand side of the above equation are linear functions of the angle averaged density matrix vector $\mathbf{g}_k$, the coefficient depending on $\mathbf{k}$ after integration over $\mathbf{k}'$. From this, we derive closed equations of motion for the charge ($N = \sum_{\mathbf{k}} g_k^0$) and spin ($S^i = \sum_{\mathbf{k}} g_k^i$ with $i = 1, 2, 3$) densities by doing the appropriate sums over $\mathbf{k}$. In the diffusive regime, $\omega\tau \ll 1$, we do a linear expansion with respect to ω and transform back from ω to t, to get the diffusion equation

$$\partial_t \begin{pmatrix} \Delta N_{\mathbf{q}} \\ S_{\mathbf{q}}^x \\ S_{\mathbf{q}}^y \\ S_{\mathbf{q}}^z \end{pmatrix} = -\mathcal{D}(\mathbf{q}) \begin{pmatrix} \Delta N_{\mathbf{q}} \\ S_{\mathbf{q}}^x \\ S_{\mathbf{q}}^y \\ S_{\mathbf{q}}^z \end{pmatrix}, \quad (36)$$

where $\Delta N_{\mathbf{q}}$ and $S_{\mathbf{q}}^i$ are, respectively, the components of the density and the spin density deviations from the (uniform) equilibrium state with wave vector $\mathbf{q}$. The 4×4 diffusion matrix $\mathcal{D}(\mathbf{q})$ is defined by

$$\mathcal{D}_{ij} = \frac{\delta_{ij}}{\tau} - \frac{1}{\tau}\langle[\mathcal{I} + (\mathcal{I} + \mathcal{K}_{\mathbf{k}'})^{-1}\mathcal{M}_{\mathbf{k}',\mathbf{k}}](\mathcal{I} + \mathcal{K}_{\mathbf{k}})^{-1}(\mathcal{I} + T_{\mathbf{k}})\rangle_{ij}$$
$$- \frac{1}{S_{\mathbf{q}}^j}\langle[(\mathcal{I} + \mathcal{K}_{\mathbf{k}})^{-1}]^{il} I_{\mathbf{k}}^{(b),l}(\tilde{\mathbf{g}}_{j\mathbf{k}}, \tilde{\mathbf{g}}_{j\mathbf{k}'})\rangle\Big|_{\omega=0}, \quad (37)$$

where $\langle.\rangle$ represents the average over the carrier distribution in momentum space and includes integration over both $\mathbf{k}$ and $\mathbf{k}'$. In the last term, $\tilde{\mathbf{g}}_{j\mathbf{k}}$ denotes the contribution to the quasiequilibrium distribution arising, in accordance with Eq. (34), from the jth component of the equilibrium density matrix $\mathbf{g}_k$, i.e., $\tilde{g}_{j\mathbf{k}}^i = [(\mathcal{I} + \mathcal{K})^{-1}(\mathcal{I} + T_{\mathbf{k}})]^{ij} g_k^j$. Thus the diffusion matrix is independent of $\mathbf{k}$ and $\mathbf{k}'$, but it does depend, via the matrices $\mathcal{K}_{\mathbf{k}}$, $\mathcal{T}_{\mathbf{k}}$ and $\mathcal{M}_{\mathbf{k},\mathbf{k}'}$ (see Appendix A) on the wave vector $\mathbf{q}$, conjugate to $\mathbf{r}$. In order to simplify the expression, we have introduced $S_{\mathbf{q}}^0 = \Delta N_{\mathbf{q}}$ in Eq. (37) for $j = 0$.

In the following, we assume $k_F q/m, |\lambda_i| k_F \ll E_F$ and do a perturbation expansion with respect to $\mathcal{T}_{\mathbf{k}}$ and $\mathcal{K}_{\mathbf{k}}$. We retain the zeroth- and first-order contributions in the extrinsic SOC parameter α'. Terms of second order in α' are retained only insofar as they are responsible for the EY spin-relaxation process. The details of the calculation are given in the Appendix B. The final equation of motion is[3]

$$\partial_t \begin{pmatrix} \Delta N_{\mathbf{q}} \\ S_{\mathbf{q}}^x \\ S_{\mathbf{q}}^y \\ S_{\mathbf{q}}^z \end{pmatrix} = -\begin{pmatrix} Dq^2 - i\mathbf{q}\cdot\mathbf{v} & -i\theta_{\text{SH}}Dq_y q_1 & -i\theta_{\text{SH}}Dq_x q_2 & -i\theta_{\text{SH}}(\mathbf{v}\times\mathbf{q})_z \\ -\theta_{\text{SH}}(v_y + iDq_y)q_1 & Dq^2 - i\mathbf{q}\cdot\mathbf{v} + \frac{1}{\tau_{sx}} & i\kappa(\mathbf{v}\times\mathbf{q})_z & (i2Dq_x + v_x)q_1 \\ -\theta_{\text{SH}}(v_x + iDq_x)q_2 & -i\kappa(\mathbf{v}\times\mathbf{q})_z & Dq^2 - i\mathbf{q}\cdot\mathbf{v} + \frac{1}{\tau_{sy}} & -(i2Dq_y + v_y)q_2 \\ -i\theta_{\text{SH}}(\mathbf{v}\times\mathbf{q})_z & -(i2Dq_x + v_x)q_1 & (i2Dq_y + v_y)q_2 & Dq^2 - i\mathbf{q}\cdot\mathbf{v} + \frac{1}{\tau_{sz}} \end{pmatrix} \begin{pmatrix} \Delta N_{\mathbf{q}} \\ S_{\mathbf{q}}^x \\ S_{\mathbf{q}}^y \\ S_{\mathbf{q}}^z \end{pmatrix}, \quad (38)$$

___

[3]We retain the leading term in each matrix element here, as well as the current matrices below.

with $q_1 = 2m\lambda_1$, $q_2 = 2m\lambda_2$, and k_F the Fermi wave vector. The dimensionless parameter $\kappa = \alpha' k_F^2$ describes the efficiency of spin current swapping, which will be discussed later. $\mathbf{v} = \tau e\mathbf{E}/m$ and $D = \tau\langle k^2/(2m^2)\rangle$ represent the

drift velocity and the two-dimensional diffusion constant, respectively.

We notice that the coupling between charge and spin degrees of freedom is controlled by a cumulative spin Hall angle, $\theta_{\text{SH}} = \theta_{\text{SH}}^{\text{ss}} + \theta_{\text{SH}}^{\text{sj}} + \theta_{\text{SH}}^{\text{int}}$, which sums up the contributions due to skew scattering, side-jump and intrinsic mechanisms:

$$\theta_{\text{SH}}^{\text{ss}} = \frac{\alpha' n_i}{2\pi} \left(\frac{m v_0}{\hbar^2} \right)^3 \frac{m D}{\hbar}, \tag{39}$$

$$\theta_{\text{SH}}^{\text{sj}} = -\frac{2\alpha' m}{\hbar \tau}, \tag{40}$$

$$\theta_{\text{SH}}^{\text{int}} = \frac{2\lambda_1 \lambda_2 m \tau}{\hbar}, \tag{41}$$

(we have reinstated $\hbar$ to highlight the dimensionless character of the spin Hall angle). However, this charge-spin coupling is asymmetric, due to the presence of the electric field, which manifests itself in the drift velocities v_x and v_y in the first column of the matrix. (To avoid misunderstanding, we point out that the spin Hall angle controls only part of the total spin Hall current: the complete spin Hall current also contains a diffusion term—see next section—which is responsible for the well-known vanishing of the spin Hall conductivity in the absence of spin-orbit coupling from impurities.) The spin-relaxation times arise from the combination of the DP and EY mechanisms:

$$1/\tau_{si} = 1/\tau_{si}^{\text{DP}} + 1/\tau_{si}^{\text{EY}}, \quad (i = x, y, z), \tag{42}$$

where, for the special case of a (001) quantum well of a zinc-blende semiconductor,

$$
\begin{aligned}
1/\tau_{sx}^{\text{DP}} &= D q_1^2, \\
1/\tau_{sy}^{\text{DP}} &= D q_2^2, \\
1/\tau_{sz}^{\text{DP}} &= D(q_1^2 + q_2^2),
\end{aligned}
\tag{43}
$$

and

$$1/\tau_{sx}^{\text{EY}} = 1/\tau_{sy}^{\text{EY}} = \left(\alpha' k_F^2 \right)^2 / \tau. \tag{44}$$

The vanishing of $1/\tau_{sz}^{\text{EY}}$ is a somewhat artificial feature of our model, in which we have assumed the impurity potential to be strictly two-dimensional and thus conserving the z component of the spin. A more realistic model, in which the impurity

potential depends also on z, would yield finite EY relaxation time in the z direction [65,66].

When $\theta_{\text{SH}} = \theta_{\text{SH}}^{\text{int}}$ and $\mathbf{E} = 0$, the above Eq. (38) reduce to those of Ref. [67]. We have thus generalized those equations to take into account not only the extrinsic mechanisms of spin Hall effect, but also the effect of the electric field.

B. Equations for the currents

The diffusion equations derived in the previous subsection correspond to a "reduction" of the full set of Eqs. (1)–(4), amounting to an elimination of the currents in favor of the densities. To complete the formalism, we must now derive the expressions for the charge and spin current densities. The "obvious" expression $\tilde{\mathbf{J}}^i = \sum_{\mathbf{k}}(1/2)\text{Tr}[\rho_{\mathbf{k}}\{\sigma^i, \nabla_{\mathbf{k}} H_{\mathbf{k}}\}]$ is incomplete, because it fails to include the anomalous velocity arising from the spin-orbit coupling with impurities. The complete and correct expression for the matrix element of the velocity between states $\mathbf{k}$ and $\mathbf{k}'$ is

$$
\begin{aligned}
\mathbf{v}_{\mathbf{k}\mathbf{k}'} &= (\nabla_{\mathbf{k}} H_{\mathbf{k}}) \delta_{\mathbf{k}\mathbf{k}'} - i[H_U, \mathbf{r}]_{\mathbf{k}\mathbf{k}'} \\
&= (\nabla_{\mathbf{k}} H_{\mathbf{k}}) \delta_{\mathbf{k}\mathbf{k}'} - i\alpha' \boldsymbol{\sigma} \times (\mathbf{k} - \mathbf{k}') v_0.
\end{aligned}
\tag{45}
$$

The current due to the last term on the right-hand side can be calculated from the "off-diagonal" density matrix $\rho_{\mathbf{k}'\mathbf{k}} \simeq i\pi v_0 \delta(\epsilon_{\mathbf{k}} - \epsilon_{\mathbf{k}'})(\rho_{\mathbf{k}'} - \rho_{\mathbf{k}})$, which is zeroth order in spin-orbit coupling and first order in the impurity potential. After some simplification, the corresponding contribution is cast in the relaxation time approximation form:

$$\tilde{\mathbf{J}}'^i = \frac{\alpha'}{\tau} \sum_{\mathbf{k}} (1/2)\text{Tr}[\rho_{\mathbf{k}}\{\sigma^i, \mathbf{k} \times \sigma\}], \tag{46}$$

and the complete current is

$$\mathbf{J}^i = \tilde{\mathbf{J}}^i + \tilde{\mathbf{J}}'^i = \sum_{\mathbf{k}} (1/2)\text{Tr}[\rho_{\mathbf{k}}\{\sigma^i, \tilde{\mathbf{v}}_{\mathbf{k}}\}] \tag{47}$$

with a modified velocity operator $\tilde{\mathbf{v}}_{\mathbf{k}} = \nabla_{\mathbf{k}} H_{\mathbf{k}} + (\alpha'/\tau)\mathbf{k} \times \boldsymbol{\sigma}$. We notice that this result is consistent with the calculation of the velocity from the time derivative of the "physical" position operator, discussed, for example, in Refs. [60,61,68,69]. Finally, by substituting in Eq. (47), the solution for the density matrix $\rho_{\mathbf{k}}$, we obtain the currents in terms of the densities:

$$
\begin{pmatrix} J_x^0(\mathbf{q}) \\ J_x^x(\mathbf{q}) \\ J_x^y(\mathbf{q}) \\ J_x^z(\mathbf{q}) \end{pmatrix} =
\begin{pmatrix}
-(iDq_x + v_x) & 0 & -\theta_{\text{SH}} D q_2 & \theta_{\text{SH}}(iDq_y + v_y) \\
0 & -(iDq_x + v_x) & i\kappa D q_y & D q_1 \\
0 & -i\kappa D q_y & -(iDq_x + v_x) & 0 \\
\theta_{\text{SH}}(iDq_y + v_y) & -D q_1 & 0 & -(iDq_x + v_x)
\end{pmatrix}
\begin{pmatrix} \Delta N_{\mathbf{q}} \\ S_{\mathbf{q}}^x \\ S_{\mathbf{q}}^y \\ S_{\mathbf{q}}^z \end{pmatrix},
\tag{48}
$$

$$
\begin{pmatrix} J_y^0(\mathbf{q}) \\ J_y^x(\mathbf{q}) \\ J_y^y(\mathbf{q}) \\ J_y^z(\mathbf{q}) \end{pmatrix} =
\begin{pmatrix}
-(iDq_y + v_y) & -\theta_{\text{SH}} D q_1 & 0 & -\theta_{\text{SH}}(iDq_x + v_x) \\
0 & -(iDq_y + v_y) & -i\kappa D q_x & 0 \\
0 & i\kappa D q_x & -(iDq_y + v_y) & -D q_2 \\
-\theta_{\text{SH}}(iDq_x + v_x) & 0 & D q_2 & -(iDq_y + v_y)
\end{pmatrix}
\begin{pmatrix} \Delta N_{\mathbf{q}} \\ S_{\mathbf{q}}^x \\ S_{\mathbf{q}}^y \\ S_{\mathbf{q}}^z \end{pmatrix}.
\tag{49}
$$

The details of the derivation can be found in Appendix C. Again, the coupling between charge current and spin polarization, as well as that between spin current and charge density, is found to be proportional to the total spin Hall angle θ_{SH}.

We can now verify by direct inspection that the expressions for the charge and spin currents read from Eqs. (48) and (49) agree with the phenomenological equations (3) and (4). The presence of the spin current swapping term in Eq. (4) is essential to obtain this perfect agreement, as will become evident in the discussion of Sec. V C. This gives us confidence that the spin-current swapping effect has been included properly at the phenomenological level. Moreover, by substituting Eqs. (48) and (49) into the continuity equations, i.e., Eqs. (1) and (2), we can demonstrate that the resulting drift-diffusion equations for the densities coincide with Eq. (38), proving the consistency of our theory.

V. DRIFT-DIFFUSION EQUATIONS AT WORK: HOMOGENEOUS SITUATIONS

In this section, we consider a few basic applications of the formalism to homogenous situations, for which the wave vector $\mathbf{q} = 0$. For definiteness, we consider a (001) quantum well in a semiconductor of the zinc-blende structure (e.g., GaAs) with Rashba and Dresselhaus spin-orbit interactions. The SU(2) vector potentials for this system are given in Eq. (10). The effects we study are the Edelstein effect and its inverse, the spin Hall effect and its inverse, and the spin-current swapping effect. As shown below, we can recover the well-known results on (inverse) spin Hall effect and (inverse) Edelstein effect very easily from our drift-diffusion equations, revealing the advantage of those equations. In addition, we predict the vanishing of the spin current swapping effect due to the compensation effect between external electric field and impurity potential.

A. Edelstein effect and its inverse

As a first application, consider the generation of a spin polarization from an electric field applied along the x direction. From the third equation in (38), we find that the time evolution of S_y is determined by

$$\partial_t S^y = 2m\lambda_2 \theta_{\text{SH}} v_x N - \frac{S^y}{\tau_{sy}}, \tag{50}$$

where the first term on the right-hand side is the spin-pumping generated by the partial conversion of the charge current into a transverse spin current, while the second term represents the spin-relaxation process. In the steady state, setting the time derivative of S^y to zero, one obtains the spin density

$$S^y = -2\theta_{\text{SH}} m\lambda_2 \tau_{sy} J_x^0, \tag{51}$$

where we have used $-v_x N = J_x^0$ to zeroth order in the SOC. As expected, the spin polarization vanishes for $\lambda_2 \to 0$, which corresponds to weak band SOC limit or balanced Dresselhaus and Rashba SOCs.

For the inverse process, i.e., the charge current induced by a nonequilibrium homogeneous spin-accumulation S^y, the first

equation in (48) gives

$$J_x^0 = -v_x N - 2\theta_{\text{SH}} Dm\lambda_2 S^y. \tag{52}$$

In the absence of an electric field ($v_x = 0$), we recover the known expression for the inverse Edelstein effect [46]:

$$J_x^0 = -2\theta_{\text{SH}} Dm\lambda_2 S_y. \tag{53}$$

We note that the role of "driving field" in the direct Edelstein effect is played by the electric field E_x, while in the inverse Edelstein effect, it is played by the "spin-injection field" $\dot{B}^y$ (see Ref. [46]). Thus, to check Onsager's reciprocity relations, we must compare the ratio S^y/E_x from Eq. (51) to the ratio $J_x^0/\dot{B}^y$ from Eq. (53). Substituting $J_x^0 = -eNE_x\tau/m$ in Eq. (51), and $S_y = -g\mu_B N_0 \dot{B}^y \tau_{sy}$ (Ref. [46]) in Eq. (53), where $N_0 = N/E_F$ is the two-dimensional density of states, we can readily verify that $S^y/E_x = eJ_x^0/(g\mu_B \dot{B}^y)$, showing that Onsager's reciprocity relation is fulfilled.

B. Spin Hall effect and its inverse

Next, we consider the homogeneous spin Hall effect resulting from an electric field applied along the x direction. According to the last equation in (49), the transverse spin current is given by

$$J_y^z = -\theta_{\text{SH}} v_x N + 2m\lambda_2 DS^y. \tag{54}$$

We can clearly see that, as anticipated in the previous section after Eq. (43), the spin Hall angle θ_{SH} controls only part of the spin current—a part that we refer to as "drift current." The remaining part is a "diffusion current," which arises in the SU(2) theory even in the absence of a spatial gradient of the spin density. Its physical origin is in the spin precession caused by the Rashba and Dresselhaus fields. By substituting the steady-state solution of spin polarization, i.e., Eq. (51), we arrive at the complete expression for the spin Hall spin current:

$$J_y^z = \frac{\theta_{\text{SH}}}{\left(\tau_{sy}^{\text{EY}}/\tau_{sy}^{\text{DP}}\right) + 1} J_x^0, \tag{55}$$

(again, we have used $-v_x N = J_x^0$ to zeroth order in the SOC), which correctly describes the crossover between the finite impurity-driven spin Hall conductivity in the limit of weak spin precession ($\tau_{sy}^{\text{DP}} \gg \tau_{sy}^{\text{EY}}$) and the vanishing spin Hall conductivity in the strong precession ($\tau_{sy}^{\text{DP}} \ll \tau_{sy}^{\text{EY}}$) [42].

To exhibit the inverse spin Hall effect, we consider the first of Eqs. (49), which yields, in the absence of an electric field in the y direction,

$$J_y^0 = -2\theta_{\text{SH}} Dm\lambda_1 S^x - \theta_{\text{SH}} v_x S^z. \tag{56}$$

The first term on the right-hand side is the inverse Edelstein effect current. The second term, in the leading order, can be written as $\theta_{\text{SH}} J_x^z$, where J_x^z is the spin current. We now observe, according to the second of Eqs. (38), at the steady state,

$$\frac{S^x}{\tau_{sx}} + 2m\lambda_1 v_x S^z = 0. \tag{57}$$

We can then write

$$S^x = 2m\lambda_1 \tau_{sx} J_x^z \tag{58}$$

and, by substituting in Eq. (56), get

$$J_y^0 = [1 - D(2m^2\lambda_1)^2\tau_{sx}]\theta_{SH}J_x^z$$
$$= \left(1 - \frac{\tau_{sx}}{\tau_x^{DP}}\right)\theta_{SH}J_x^z$$
$$= \frac{\theta_{SH}}{(\tau_{sy}^{EY}/\tau_{sy}^{DP}) + 1}J_x^z. \qquad (59)$$

This equation is the mathematical formulation of the inverse spin Hall effect, which converts a spin current into a perpendicular charge current. Comparison with Eq. (55) shows that the Onsager reciprocity relation is satisfied.

C. Spin-current swapping

As a final example in the homogeneous class, we discuss the spin-current swapping (SCS) effect [29], whereby a primary spin current, $[J_j^i]^{(0)}$, induces a transverse spin current in which the spin direction and the direction of flow are interchanged according to the equation

$$[J_i^j]^{SCS} = \kappa \left([J_j^i]^{(0)} - \delta_{ij}[J_l^l]^{(0)}\right). \qquad (60)$$

To observe experimentally the spin swapping effect, one might think to apply a uniform electric field E_x to a homogeneous electron liquid, with a uniform spin-polarization S^x in the x direction. This naturally creates a primary spin current $[J_x^x]^{(0)} = -v_x S^x$, which should then induce the spin current

$$[J_y^y]^{SCS} = -\kappa [J_x^x]^{(0)} = \kappa v_x S^x. \qquad (61)$$

Unfortunately, our equations demonstrate that the swapped spin current is undetectable in this homogeneous setup, because it is exactly canceled by the SU(2) diffusion current arising from the spin precession in the spin-orbit field generated by the electric field E_x. This cancellation is already evident from the fact that the matrix elements containing κ in Eqs. (48) and (49) vanish in a homogeneous situation, because $\mathbf{q} = 0$. However, our phenomenological Eq. (4) gives more insight into the underlying physics. The SOC effective magnetic field due to the in-plane external electric field is in the same direction (z direction) as that from the impurity and both contribute to the SCS. The SCS term on the right-hand side of Eq. (4) takes into account only the effect of the impurity, which, in this case, is given by Eq. (61). The additional effect of the electric field, due to the vector potential A_y^z in Eq. (10), is taken into account by the covariant derivative in Eq. (4). The two contributions cancel each other exactly for essentially the same reasons that lead to the cancellation (on the average) of the force exerted by the electric field against the force exerted by the impurities on the electrons in a steady state situation.

In order to observe the spin-current swapping effect in an experiment, one should avoid the influence from electric-field-induced SOC. One way to achieve this is to inject the spin current by optical means. Another possibility is to inject a pure spin current via the spin Seebeck effect [70] or via multiterminal electrical spin injection techniques [71]. We will return to this point in Sec. VI E.

VI. DRIFT-DIFFUSION EQUATIONS AT WORK: INHOMOGENEOUS SITUATIONS

Let us now consider some applications of our theory to inhomogeneous situations. We have in mind, specifically, the electron-hole density waves and spin density waves, which can be optically induced on the surface of a semiconductor quantum well through the interference of laser beams coming from different directions with different polarizations. These structures are also referred to as "gratings," because the nonuniformity of the densities causes a modulation in the refractive index of the electron gas. The spin density generated in this manner is typically associated with the electrons only (the holes losing their polarization during a very short relaxation time) and is perpendicular to the plane of the quantum well. Recently, developed pump-probe techniques have allowed detailed studies of the spontaneous dynamical evolution of these systems on a picosecond time scale: by this we mean that it is possible to record the density, the spin density and the overall velocity of propagation of the grating on a picosecond scale. Through such experiments it has been possible, for example, to establish the presence of a long-lived "persistent spin helix" in nearly balanced (001) quantum wells (i.e., quantum wells with $\alpha \simeq \pm\beta$), and to demonstrate interesting effects related to Coulomb drag in spin diffusion and electron-hole diffusion.

In this section, we focus on the partial conversion of an electron-hole density grating into an electronic spin density wave under the action of an electric field, which we choose, for definiteness, to be parallel to the x axis: $\mathbf{E} = E\hat{x}$. In addition to the experimentally observed Doppler effect, we also predict several interesting phenomena, such as periodic Edelstein effect and collective spin Hall effect. The numerical calculations are carried out for a 10-nm GaAs QW grown in (001) direction, in which the Dresselhaus coefficient $\beta = 10$ meV Å, unless otherwise specified. The Rashba coefficient α is assumed to be tunable via gate voltage. The Elliott-Yafet spin-relaxation process is neglected.

In Fig. 2, we plot the magnitudes of the three components of the homogeneous spin Hall drift velocity $v^{ss} = \theta_{SH}^{ss}v$, $v^{sj} = \theta_{SH}^{sj}v$, and $v^{int} = \theta_{SH}^{int}v$ as functions of momentum relaxation time. The latter is varied by changing the concentration of impurities. Here, v is the standard drift velocity of the electrons given by $v = \mu E$, where $\mu \simeq e\tau/m$ is the mobility, whose value is shown on the upper axis of Fig. 2. Qualitatively, the side jump drift velocity is independent of momentum relaxation time, whereas the intrinsic spin Hall drift velocity and the skew scattering spin Hall drift velocity are proportional to τ^2 (provided $\tau \ll \tau_{DP}$) and τ, respectively. It is seen that the spin Hall drift velocities due to the side-jump effect and the skew scattering are comparable when the mobility is below 0.1 m^2 V^{-1} s^{-1}, while the skew scattering is dominant in an intermediate regime. In the high-mobility region, the relative contribution of skew scattering and intrinsic mechanism can be effectively controlled by changing the Rashba coefficient. This can be easily understood from $v^{int} = 2\tau m(\beta^2 - \alpha^2)v$, which demonstrates the vanishing of the intrinsic mechanism for $\alpha = \pm\beta$. In the following, we consider a few situations of experimental interest, in which an electric field is applied to a
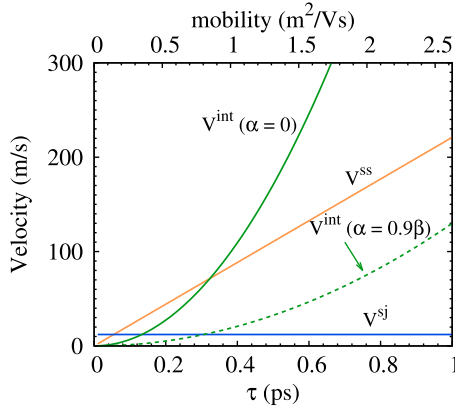
FIG. 2. (Color online) Magnitudes of spin Hall velocities due to skew scattering (v^{ss}), side jump (v^{sj}), and intrinsic mechanism (v^{int}) as functions of momentum relaxation time (lower axis) and mobility (upper axis) in 10-nm GaAs QW grown in (001) direction with electron density $n_e = 10^{12}$ cm^{-2}. The electric field is taken to be 1 kV/cm. The results for the intrinsic mechanism are computed with two different values of Rashba coefficient.

density or a spin density grating, parallel or perpendicular to the direction of the wave vector.

A. Density grating with q∥E: periodic Edelstein effect

Let us begin with the case in which the system is initially prepared in a density wave state (no spin density), with the wave vector of the electron-hole density wave parallel to the direction x of the external electric field. From the drift-diffusion equations (38), we see that only the y component of the spin density is coupled to the particle density:

$$\partial_t \Delta N_{\mathbf{q}} = (iqv - D_a q^2)\Delta N_{\mathbf{q}} + i\theta_{SH} D_s q q_2 S_{\mathbf{q}}^y, \quad (62)$$

$$\partial_t S_{\mathbf{q}}^y = \left[iqv - D_s\left(q^2 + q_2^2\right)\right]S_{\mathbf{q}}^y + \theta_{SH}(iD_s q + v)q_2 \Delta N_{\mathbf{q}}. \quad (63)$$

The spin density coupling strength is proportional to $\theta_{SH}q_2$, where $q_2 \equiv 2m\lambda_2 = 2m(\beta - \alpha)$, and therefore it vanishes in the balanced case $\alpha = \beta$.

Notice that we have replaced the plain diffusion constant D by the ambipolar diffusion constant D_a for the electron-hole density grating and by the spin diffusion D_s for the spin grating [36]. The first replacement takes into account the almost perfect screening of the space charge that occurs when electrons and holes diffuse together in an electron-hole density wave [33,36,72]. The second takes the effect of spin Coulomb drag, which reduces the spin diffusion constant relative to standard D [32,73–76].

Neglecting the feedback from spin grating to density grating, i.e., the second term on the right-hand side in Eq. (62), which is of second order in spin-Hall angle, we find that the density evolves according to the standard analytic formula

$$\Delta N_{\mathbf{q}} = A_0 e^{(iqv - D_a q^2)t + iqx}, \quad (64)$$

where A_0 is the amplitude of the initial electron-hole density grating. Substituting this in the equation for the spin density, we obtain an analytically solvable equation whose solution is

$$S_{\mathbf{q}}^y = \frac{A_0\theta_{SH}(iD_s q + v)q_2 \exp[iq(x + vt)]}{D_s\left(q^2 + q_2^2\right) - D_a q^2}$$

$$\times \left\{\exp(-D_a q^2 t) - \exp\left[-D_s\left(q^2 + q_2^2\right)t\right]\right\}. \quad (65)$$

In the absence of the electric field ($v = 0$), the density grating simply decays at a rate $D_a q^2$ determined by the ambipolar diffusion constant. The spatially periodic diffusion current generates a spin polarization in the y direction—an effect that can be viewed as the analog of the uniform Edelstein effect except that (i) it is spatially periodic and (ii) it is driven by a diffusion current. This polarization, starting from zero at the initial time, reaches a maximum at time $t = \ln[D_s(q^2 + q_2^2)/(D_a q^2)]/[D_s(q^2 + q_2^2) - D_a q^2]$ before eventually tending to zero at long times, when the density grating disappears.

When the electric field is applied, the phase of the grating acquires a linear variation in time, corresponding to a drift with velocity v in the direction of the electric field. The y component of the spin polarization also drifts with the same velocity v. Thus the periodic Edelstein effect offers a way to generate a drifting in plane-polarized spin grating: this would be difficult, if not impossible, to produce by optical means.

B. Spin grating with q∥E: helical Doppler effect

To exhibit the dynamics of an optically created spin grating polarized along z direction, we write the drift-diffusion equations in terms of the two helical modes $S_{\mathbf{q}}^\pm = (S_{\mathbf{q}}^x \pm iS_{\mathbf{q}}^z)/\sqrt{2}$,

$$\partial_t S_{\mathbf{q}}^\pm = \left[i(q \pm q_1)v - D_s(q \pm q_1)^2 + D_s q_1^2 - \frac{1}{\tau_s^+}\right]S_{\mathbf{q}}^\pm - \frac{S_{\mathbf{q}}^\mp}{\tau_s^-} \quad (66)$$

where $1/\tau_s^\pm = (1/\tau_{sx} \pm 1/\tau_{sz})/2$ and $q_1 = 2m\lambda_1$. For $|\lambda_1| \gg |\lambda_2|$, we can neglect the coupling between the two modes ($\propto 1/\tau_s^-$), which leads us to the analytic solution

$$S_{\mathbf{q}}^\pm = (\pm iA_z/\sqrt{2})\exp[iqx + i(q \pm q_1)vt - D_s(q \pm q_1)^2 t], \quad (67)$$

where the two spin helical modes show different phase evolutions, with phases $\phi_\pm = (q \pm q_1)vt$. Here, A_z is the amplitude of the initial spin grating. We see that the "Doppler shifts" are different for the two helical components. Recall that the helical mode S^- describes the "persistent spin helix" in the balanced case [34,77–82], when the wave vector q of the grating matches the SOC wave vector q_1. In recent experiments by Yang *et al.* [33,47], the time evolution of the spatial phase has been measured by Doppler velocimetry. It is easy to see that, on a short time scale, when the exponential in the above equation can be linearized, the superposition of the two helical modes with comparable amplitudes leads to a global phase velocity $\dot{\phi} \simeq (\dot{\phi}_+ + \dot{\phi}_-)/2 \simeq qv$, which is the same as in Eq. (65). However, on a long-time scale,

only the long-lived mode S^-, which corresponds to the persistent spin helix, is relevant (assuming, of course, that q is close to q_1) leading to $\dot{\phi} \simeq \dot{\phi}_- \simeq (q - q_1)v$, which can have positive or negative sign depending on the whether $q > q_1$ or $q < q_1$ (Refs. [50,83,84]). The switching sign of the phase velocity has been experimentally observed and provides strong evidence for the existence of a long-lived spin helix in this system [47].

$$
\begin{pmatrix}
Dq^2 & -i\theta_{\mathrm{SH}}Dqq_1 & 0 & -i\theta_{\mathrm{SH}}vq \\
-i\theta_{\mathrm{SH}}Dqq_1 & D(q^2+q_1^2) & 0 & vq_1 \\
-\theta_{\mathrm{SH}}vq_2 & 0 & D(q^2+q_2^2) & -2iDqq_2 \\
-i\theta_{\mathrm{SH}}vq & -vq_1 & 2iDqq_2 & D(q^2+q_1^2+q_2^2)
\end{pmatrix}. \tag{68}
$$

Let us first consider the case in which the band SOC is zero (this is the case for a GaAs (110) quantum well, see Ref. [36]). Then both S^x and S^y are decoupled from the density grating, and the solution for the S^z component is given by

$$
S^z = \frac{i A_0 \theta_{\mathrm{SH}} v \exp(iqy)}{(D_s - D_a)q}[\exp(-D_a q^2 t) - \exp(-D_s q^2 t)], \tag{69}
$$

with the spin Hall angle θ_{SH} being entirely due to electron-impurity scattering, i.e., of entirely extrinsic origin. Here we are neglecting, for simplicity, the small electron-hole recombination rate Γ, which would modify the decay rate of density grating from $D_a q^2$ to $D_a q^2 + \Gamma$ (Ref. [36]). A nonzero value of $\Gamma \simeq 1$ ns^{-1} is, however, included in the calculations plotted in Fig. 3. The spin density from Eq. (69) vanishes both at short times ($t \to 0$), when the electric field has not had sufficient time to produce its effect, and for long times ($t \to \infty$)
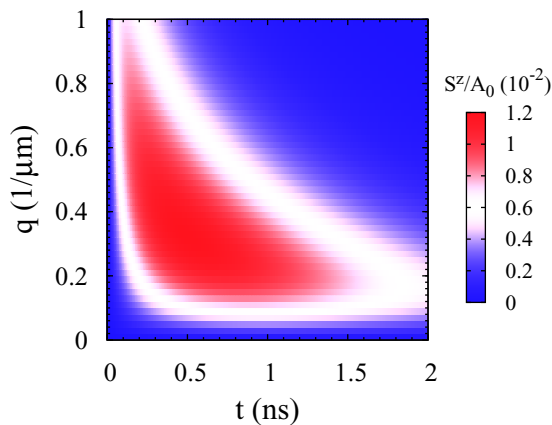

FIG. 3. (Color online) Time evolution of the amplitude of the spin grating S^z arising from an electron-hole grating of wave vector q in the presence of an electric field perpendicular to the wave vector. Here only the extrinsic spin Hall effect (skew scattering and side-jump effect) is considered. The largest amplitude of the spin grating occurs in the central region of the plot (in red), and is maximized about $q = 0.2$ μm^{-1}. In this section, we take $\tau = 1$ ps, $D_a = 20$ cm^2/s, and $D_s = 200$ cm^2/s unless otherwise specified. The electron-hole recombination rate $\Gamma = 1$ ns^{-1} is used.

C. q ⊥ E: collective spin Hall effect, extrinsic

When **q** is perpendicular to the external electric field, an electron-hole density grating becomes coupled, via the spin Hall effect, to the z component of the spin density. This coupling generates a spin density grating polarized in the z direction, which can be observed in a Kerr/Faraday rotation measurement. The diffusion matrix $\mathcal{D}$ in this configuration turns to be

when the original density grating has diffused away. Its maximum amplitude occurs at $t = \ln(D_a/D_s)/[(D_a - D_s)q^2]$ and is given by

$$
\frac{A_{S_z}^{\max}(q)}{A_0} = \frac{\theta_{\mathrm{SH}}v}{D_a q}\left(\frac{D_s}{D_a}\right)^{D_s/(D_a-D_s)}, \tag{70}
$$

which is approximately the fraction of the grating wavelength $\sim 1/q$ through which the electrons move, with drift velocity $\theta_{\mathrm{SH}}v$, during the grating lifetime $\sim 1/D_a q^2$. In Fig. 3, we plot the time evolution of the amplitude of the induced spin grating as a function of wave vector. In this figure, the optimal value of q, leading to the largest amplitude of the induced spin grating, is about $q^{\mathrm{opt}} \sim 0.2$ μm^{-1}, which is not too far from experimentally realized values [32,33].

D. q ⊥ E: collective spin Hall effect, intrinsic

Let us now consider the interesting case in which the collective spin Hall effect occurs in the presence of band SOC and Rashba coupling. We will consider three cases: (i) the SOC balanced case with $\alpha = -\beta$ ($q_1 = 0$ and $q_2 = q_0$ with $q_0 = 4m\beta/\hbar^2$), (ii) the SOC balanced case with $\alpha = \beta$ ($q_1 = q_0$ and $q_2 = 0$), and (iii) the generic $\alpha \neq \pm\beta$ case.

(i) In the SOC balanced case with $\alpha = -\beta$, the x component of the spin decouples from the rest, while the S^y and S^z components remain coupled to the density and to each other. Transforming to the helical basis, $S^{\pm} = (S^y \pm iS^z)/\sqrt{2}$, we obtain

$$
\partial_t \Delta N_{\mathbf{q}} = -D_a q^2 (\Delta N_{\mathbf{q}}) + \theta_{\mathrm{SH}}vq\frac{(S_{\mathbf{q}}^+ - S_{\mathbf{q}}^-)}{\sqrt{2}}, \tag{71}
$$

$$
\partial_t S_{\mathbf{q}}^+ = (\theta_{\mathrm{SH}}/\sqrt{2})q_- v(\Delta N_{\mathbf{q}}) - D_s q_-^2 S_{\mathbf{q}}^+, \tag{72}
$$

$$
\partial_t S_{\mathbf{q}}^- = (\theta_{\mathrm{SH}}/\sqrt{2})q_+ v(\Delta N_{\mathbf{q}}) - D_s q_+^2 S_{\mathbf{q}}^-, \tag{73}
$$

where $q_{\pm} \equiv q_0 \pm q$. From the last two equations, we see that the electric field "pumps" the spin helical modes S^+ and S^- at a rate proportional to q_- and q_+, respectively. At the same time, the diffusion process causes these modes to decay at rates $D_s q_-^2$ and $D_s q_+^2$, respectively. As before, we discard the small feedback of the spin on the evolution of the electron-hole

density. Then taking the density from Eq. (64), but without the drift term (because $\mathbf{q} \perp \mathbf{E}$), we easily obtain an analytic solution for the helical modes:

$$S_{\mathbf{q}}^{\pm} = \frac{A_0 \theta_{SH} v q_{\mp} \exp(iqy)}{\sqrt{2}(D_s q_{\mp}^2 - D_a q^2)} [\exp(-D_a q^2 t) - \exp(-D_s q_{\mp}^2 t)].$$

(74)

Interestingly, at the special wave vectors $q = \pm q_0$, for which a persistent spin helix is expected to appear in the S^+ channel (if $q = q_0$), or in the S^- channel (if $q = -q_0$) the present result shows that only the short-lived spin mode is generated, i.e., only S^- if $q = q_0$, or only S^+ if $q = -q_0$. The reason for this somewhat counterintuitive behavior is that pumping the persistent helical mode is equivalent, modulo an SU(2) rotation, to pumping a uniform spin polarization in the z direction of the rotated frame. However, the SU(2) rotation in question eliminates the band SOC, leaving only an extrinsic SOC which cannot change the spin polarization in the z direction and therefore cannot "pump" the long-lived mode [36].

The time evolution of the S^z grating amplitude is plotted in Fig. 4(a) for different magnitudes of the wave vector. Observe the change in the sign of the amplitude of the spin grating around $q = q_0$ in the long-time regime. This is because, when the grating wave vector exactly equals q_0, only the short-lived chiral mode, of which the amplitude is negligibly small after 100 ps, can be pumped by spin Hall effect [also see Fig. 4(c), where we show the S^z spin profile at different times]. For a wave vector slightly above or below q_0, the long-lived mode is also pumped, and inevitably becomes dominant after a few tens of picoseconds. According to Eq. (74), the amplitude of the pumped long-lived-mode changes sign from $q > q_0$ to $q < q_0$ and vanishes at $q = q_0$. In Figs. 4(b) and 4(d), we plot the spin configurations for two typical wave vectors, $q = 1.05q_0$ and $q = 0.95q_0$. At short times, the short-lived component of the response dominates, leading to similar behaviors in the two cases. At long times, only the long-lived mode components survive, leading to responses of opposite sign.

(ii) In the SOC balanced case with $\alpha = \beta$, it is the coupling between S^y and the other densities that vanishes. Then, the equation of motions for helical modes $S_{\mathbf{q}}^{\pm} = (S_{\mathbf{q}}^x \pm i S_{\mathbf{q}}^z)/\sqrt{2}$ takes the form

$$\partial_t S_{\mathbf{q}}^{\pm} = \frac{\theta_{SH}}{\sqrt{2}} (i D_s q_0 \mp v) q (\Delta N_{\mathbf{q}}) - [D_s(q^2 + q_0^2) \mp i v q_0] S_{\mathbf{q}}^{\pm}.$$

(75)

Note that the pumping and decay rates are the same for the amplitudes of the two modes, determined by $\theta_{SH} q (\Delta N) \sqrt{v^2 + (D_s q_0)^2}$ and $D_s(q^2 + q_0^2)$, respectively, whereas their phases are different. The time evolution of the amplitude of the S^z component is shown in Fig. 5(a). The spin profiles with $q = q_0$ at different times are shown in Fig. 5(b).

(iii) For $\alpha \neq \pm \beta$, all the spin components are coupled together, which makes the analysis much more complicated. Since the intrinsic mechanism is switched on, the collective spin Hall effect can produce large-amplitude spin gratings in a high mobility sample, see Fig. 6, where the Rashba coupling is excluded. Again, spin relaxation restricts the opportunity for observation to a relatively short time window immediately
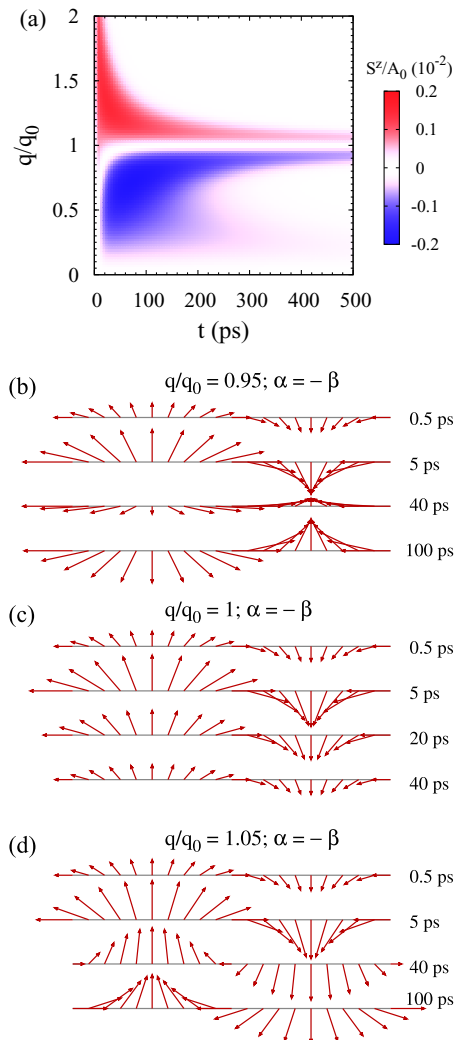

FIG. 4. (Color online) (a) Time evolution of the amplitude of the spin grating S^z arising from an electron-hole grating of wave vector q (normalized by $q_0 \simeq 3.5\ \mu\text{m}^{-1}$) in the presence of an electric field perpendicular to the wave vector with $\alpha = -\beta$. (b)–(d) The corresponding spin profiles S^y-S^z induced by collective spin Hall effect with different grating wave vectors around q_0. Four typical times are chosen for each case. For $q \neq q_0$, the profile at short time is a superposition of S^+ and S^- with weights $q - q_0$ (large) and $q + q_0$ (small). At long time, only the S^+ mode ($\propto q - q_0$) survives. (c) For $q = q_0$, the long-lived mode disappears and the long-time spin profile is qualitatively similar to the short-time state.

following the initial creation of the electron-hole density grating.

E. Spin-current swapping again

We conclude this section by showing how the spin-current swapping effect, which vanishes in the homogeneous situation of Sec. V C, can be observed in an inhomogeneous situation, such as the one proposed by Lifshitz and D'yakonov in Ref. [29]. At variance with Sec. V C, we assume that a spin current J_x^x is injected into an *unpolarized* 2DEG in a (001) quantum well, coming from a ferromagnetic electrode polarized along the x axis. In the vicinity of the contact
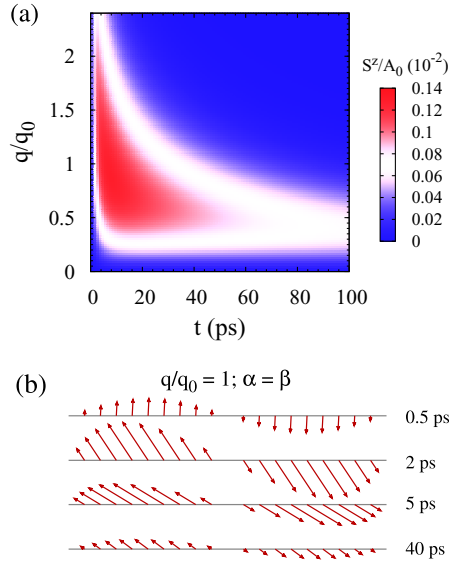
FIG. 5. (Color online) (a) Time evolution of the amplitude of the spin grating S^z arising from an electron-hole grating of wave vector q in the presence of an electric field perpendicular to the wave vector with $\alpha = \beta$. (b) The corresponding spin profiles S^x-S^z induced by collective spin Hall effect at $q = q_0$. We observe that the helical modes S^+ and S^- have the same lifetime and amplitude.

an inhomogeneous spin accumulation S^x is induced, which decays on the scale of the spin-diffusion length (we neglect the ferromagnetic proximity effect). The inhomogeneous spin accumulation drives an additional diffusion spin current, which must be added to the drift spin-current considered in Sec. V C. For simplicity, we ignore the intrinsic SOC, i.e., we set $\lambda_1 = \lambda_2 = 0$. However, we retain the SOC with the electric field E_x [given by A_y^z in Eq. (10)] and, of course, the spin-current swapping term due to extrinsic impurities. From Eq. (4), after expanding the covariant derivative and setting $v_y = 0$ and $S^y = S^z = 0$, we obtain

$$J_x^x = -(v_x + D\partial_x)S^x - \kappa J_y^y$$
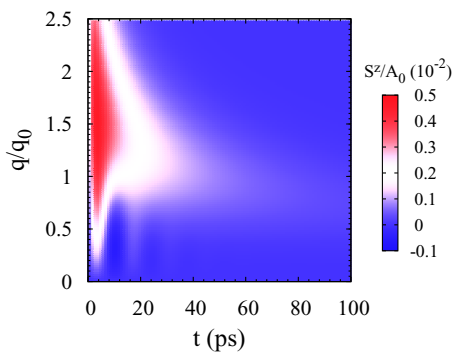$$J_y^y = -2Dm\alpha'eE_xS^x - \kappa J_x^x . \tag{76}$$

FIG. 6. (Color online) Time evolution of the amplitude of the spin grating S^z arising from an electron-hole grating of wave vector q in the presence of an electric field perpendicular to the wave vector without Rashba SOC.

Noting that $-2Dm\alpha'eE_x = -\kappa v_x$, we rewrite the second equation as

$$J_y^y = -\kappa\left(v_xS^x + J_x^x\right). \tag{77}$$

Solving the coupled equations for J_x^x and J_y^y yields

$$J_x^x = -v_xS^x - \frac{D}{1-\kappa^2}\partial_xS^x,$$
$$J_y^y = \frac{\kappa D}{1-\kappa^2}\partial_xS^x . \tag{78}$$

Thus the J_x^x component of the spin current remains, up to first order in κ equal to the primary current injected by the ferromagnetic electrode. However, the spin-current swapping effect manifests itself in the appearance of a J_y^y component of the spin current, which is proportional to the diffusion part of the primary spin current: $J_y^y \simeq \kappa D\partial_xS^x$. This should be observable.

VII. SUMMARY

We have derived the microscopic spin kinetic equation in periodically modulated two dimensional electron liquids from nonequilibrium Green's function approach. We include the spin-orbit couplings due not only to the band structure but also to the external electric field and the (nonmagnetic) impurities. Starting from the solution of the spin kinetic equation obtained from a perturbation expansion in the relaxation time approximation, we have derived a set of complete drift-diffusion equations for the charge and spin densities, in the presence of an external electric field and a grating wave vector in arbitrary directions. We find that in the drift-diffusion equations the three mechanisms of spin Hall effect, i.e., skew scattering, side jump, and the intrinsic mechanism, can be combined together into a single spin Hall angle. Moreover, we also derive explicit expressions for the charge current and the spin current and, by combining them with the drift-diffusion equations, we analyze Edelstein effect, spin Hall effect and their inverses, as well as the spin current swapping effect. We then apply our theory to the study of spin and density gratings in GaAs quantum wells. We recover the results of Doppler velocimetry experiments when the grating wave vector is parallel to the external electric field. For the grating wave vectors perpendicular to the electric field, we predict the conversion from electron-hole density grating to spin grating due to spin Hall effect. We show that single-spin-helical-mode pumping can be realized via spin Hall effect in (001) GaAs quantum well with identical Rashba and Dresselhaus coefficients. We also show that the spin-current-swapping effect vanishes in a homogeneous situation, but can be detected in a spin injection experiment.

Missing from the analysis is the effect of electron-electron scattering on the spin conductivity and the spin diffusion constant (the so-called spin Coulomb drag [32,75,76]). This can be included without difficulty: the connection between spin currents and electric fields in a spin-polarized interacting electron gas will be considered elsewhere. Finally, we note that it will be interesting to apply the present formalism to the theoretical analysis of surface acoustic wave experiments as done recently in Ref. [85].

APPENDIX A: MATRICES IN EQ. (33)

Including spin precession, diffusion and drift terms, $\mathcal{K}_\mathbf{k}$ reads

$$
\mathcal{K}_\mathbf{k} = \begin{pmatrix} \Omega & i\lambda_2\tau q_y & i\lambda_1\tau q_x & im\alpha'(\mathbf{q}\times\mathbf{v})_z \\ i\lambda_2\tau q_y & \Omega & -2B_z\tau & 2B_y\tau \\ i\lambda_1\tau q_x & 2B_z\tau & \Omega & -2B_x\tau \\ im\alpha'(\mathbf{q}\times\mathbf{v})_z & -2B_y\tau & 2B_x\tau & \Omega \end{pmatrix},
$$

(A1)

where $\Omega = -i\omega\tau + i\frac{\tau}{m}\mathbf{k}\cdot\mathbf{q} - e\tau\mathbf{E}\cdot\nabla_\mathbf{k}$ with ω and $\mathbf{q}$ being the Fourier conjugate variables with respect to t and $\mathbf{r}$. Note that the spin-spin coupling components actually show the precession effect due to the effective SOC field, which has components $B_x = -k_y\lambda_2$, $B_y = -k_x\lambda_1$, $B_z = -e\alpha'(\mathbf{k}\times\mathbf{E})_z$.

The second matrix, $\mathcal{T}_\mathbf{k}$, which describes the energy correction due to SOC, shows the density-spin coupling from the collision term $I_\mathbf{k}^{(a)}$ and $I_\mathbf{k}^{(c)}$ as

$$
\mathcal{T}_\mathbf{k} = \begin{pmatrix} 0 & -B_x\partial_{\epsilon_k} & -B_y\partial_{\epsilon_k} & -2B_z\partial_{\epsilon_k} \\ -B_x\partial_{\epsilon_k} & 0 & 0 & 0 \\ -B_y\partial_{\epsilon_k} & 0 & 0 & 0 \\ -2B_z\partial_{\epsilon_k} & 0 & 0 & 0 \end{pmatrix}.
$$

(A2)

Note that one half of the coupling between the density and the spin component along the z direction comes from $I_\mathbf{k}^{(a)}$, while the other half comes from $I_\mathbf{k}^{(c)}$ as mentioned in the main text.

The matrix $\mathcal{M}_{\mathbf{k},\mathbf{k}'}$, depending on the relative angle between the incoming momentum and the outgoing momentum in an electron-impurity scattering process, has three contributions. The first piece comes from the second term in $I_\mathbf{k}^{(0)}$ [see Eq. (23)], corresponding to the spin current swapping term, which leads to

$$
\mathcal{M}_{\mathbf{k},\mathbf{k}'}^{\text{sw}} = \alpha'\begin{pmatrix} 0 & 0 & 0 & 0 \\ 0 & 0 & -2(k_xk_y'-k_yk_x') & 0 \\ 0 & 2(k_xk_y'-k_yk_x') & 0 & 0 \\ 0 & 0 & 0 & 0 \end{pmatrix}.
$$

(A3)

The second piece, coming from the third term in $I_\mathbf{k}^{(0)}$, can be expressed as

$$
\mathcal{M}_{\mathbf{k},\mathbf{k}'}^{\text{inh}} = \alpha'\begin{pmatrix} 0 & 0 & 0 & i[\mathbf{q}\times(\mathbf{k}-\mathbf{k}')]_z \\ 0 & 0 & 0 & 0 \\ 0 & 0 & 0 & 0 \\ i[\mathbf{q}\times(\mathbf{k}-\mathbf{k}')]_z & 0 & 0 & 0 \end{pmatrix},
$$

(A4)

where the superscript "inh" suggests that this term reflects the effect of the spatial inhomogeneity during the scattering. The last contribution corresponds to the skew scattering $I_\mathbf{k}^{\text{ss}}$ [Eq. (24)] resulting in

$$
\mathcal{M}_{\mathbf{k},\mathbf{k}'}^{\text{ss}} = \alpha_{ss}\begin{pmatrix} 0 & 0 & 0 & -(k_xk_y'-k_yk_x') \\ 0 & 0 & 0 & 0 \\ 0 & 0 & 0 & 0 \\ -(k_xk_y'-k_yk_x') & 0 & 0 & 0 \end{pmatrix},
$$

(A5)

with $\alpha_{ss} = \tau n_i\alpha'(mv_0)^3(2\pi m)^{-1}$. Thus the matrix $\mathcal{M}_{\mathbf{k},\mathbf{k}'}$ in Eq. (33) is expressed by

$$
\mathcal{M}_{\mathbf{k},\mathbf{k}'} = \mathcal{M}_{\mathbf{k},\mathbf{k}'}^{\text{sw}} + \mathcal{M}_{\mathbf{k},\mathbf{k}'}^{\text{inh}} + \mathcal{M}_{\mathbf{k},\mathbf{k}'}^{\text{ss}}.
$$

(A6)

Notice that $\mathcal{M}_{\mathbf{k},\mathbf{k}'}$ is proportional to α'. In our kinetic equation (33), $I_\mathbf{k}^{(b)}$ is not written in the form of a matrix, because, as explained in Sec. III, the relaxation time approximation is inapplicable to it.

APPENDIX B: DERIVATION OF THE DRIFT-DIFFUSION EQUATIONS FOR THE DENSITIES

In this section, we present the details of the derivation of the drift-diffusion equations for the densities. Intuitively, the total diffusion matrix in Eq. (37) can be separated into two parts, the intrinsic part and the extrinsic one, according to the extrinsic SOC parameter α'. That is

$$
\mathcal{D} = \mathcal{D}^{\text{int}} + \mathcal{D}^{\text{ext}},
$$

(B1)

where the intrinsic contribution $\mathcal{D}^{\text{int}}$ corresponds to the zeroth-order term in α', equal to $\mathcal{D}_{\alpha'=0}$. The extrinsic part $\mathcal{D}^{\text{ext}}$ in principle contains all high-order contributions in α', however, because of the small value of α', it is sufficient to include only the first-order term.

Specifically, the intrinsic diffusion matrix is given by

$$
D^{\text{int}} = (1/\tau)[\mathcal{I} - \langle(\mathcal{I}+\mathcal{K}_\mathbf{k})^{-1}(\mathcal{I}+\mathcal{T}_\mathbf{k})\rangle]_{\omega=0,\alpha'=0}. \quad \text{(B2)}
$$

In the presence of an external electric field and a grating modulation, there are three scale parameters with the units of a wave vector, i.e., $q_{x,y}$, $v_{x,y}/D$, and $2m\lambda_{1,2}$. $1/q$ is the grating wave length. $l_E \equiv D/v$ is the length scale over which the electric field changes the energy of an electron by a quantity comparable to the Fermi energy; in the diffusive regime, we require the mean free path to be much smaller than this length, i.e., $v_F\tau \ll l_E$. $l_{SO} \equiv 1/(m\lambda)$ is the length scale over which the spin of an electron traveling at the Fermi velocity completes a full round of precession in the spin-orbit field. In the diffusive regime, the Dyakonov-Perel spin-relaxation time, which is the

time over which electrons diffuse on the length l_{SO}, must be much longer than the elastic scattering time. This requires that the mean free path must be much smaller also of this length $v_F \tau \ll l_{SO}$. This also means that the spin-orbit splitting is small with respect to the disorder-induced broadening of the electron states. In order to make our theory applicable for general values of the ratios between these scale parameters, we treat them on equal footing in the calculation and define a characteristic inverse length scale $l^{-1} \equiv \max(q_{x,y}, l_E^{-1}, l_{SO}^{-1})$ as the largest of the three wave vectors. Hence the diffusive limit is defined by the condition $v_F \tau \ll l$. Furthermore, the assumption of a weakly disordered Fermi gas requires the

condition $E_F \tau \gg 1$, which corresponds to a mean free path much larger than the Fermi wave length. The above inequalities are then used to carry out a perturbation expansion with respect to $\mathcal{T}_{\mathbf{k}}$ and $\mathcal{K}_{\mathbf{k}}$. We find that the leading order of the density-density and spin-spin couplings is given by l^{-2}, while the first nonvanishing spin density couplings are of the order of l^{-4}. Specifically, the spin-spin and density-density couplings are given by $\langle -\mathcal{K}_{\mathbf{k}}^2 \rangle$ and the spin density couplings are carried by $\langle \mathcal{K}_{\mathbf{k}}^3 + \mathcal{K}_{\mathbf{k}}^3 \mathcal{T}_{\mathbf{k}} \rangle$ (the lowest-order terms $\langle \mathcal{K}_{\mathbf{k}} \rangle$ and $\langle \mathcal{K}_{\mathbf{k}} \mathcal{T}_{\mathbf{k}} \rangle$ cancel against each other). Collecting all the relevant contributions in the leading order, we obtain the diffusion matrix due to the intrinsic mechanism:

$$
\mathcal{D}^{\mathrm{int}} = \begin{pmatrix}
Dq^2 - i\mathbf{q}\cdot\mathbf{v} & -i\theta_{\mathrm{SH}}^{\mathrm{int}} Dq_y q_1 & -i\theta_{\mathrm{SH}}^{\mathrm{int}} Dq_x q_2 & -i\theta_{\mathrm{SH}}^{\mathrm{int}}(\mathbf{v}\times\mathbf{q})_z \\
-\theta_{\mathrm{SH}}^{\mathrm{int}}(v_y + iDq_y)q_1 & Dq^2 - i\mathbf{q}\cdot\mathbf{v} + \frac{1}{\tau_{sx}^{\mathrm{DP}}} & 0 & (i2Dq_x + v_x)q_1 \\
-\theta_{\mathrm{SH}}^{\mathrm{int}}(v_x + iDq_x)q_2 & 0 & Dq^2 - i\mathbf{q}\cdot\mathbf{v} + \frac{1}{\tau_{sy}^{\mathrm{DP}}} & -(i2Dq_y + v_y)q_2 \\
-i\theta_{\mathrm{SH}}^{\mathrm{int}}(\mathbf{v}\times\mathbf{q})_z & -(i2Dq_x + v_x)q_1 & (i2Dq_y + v_y)q_2 & Dq^2 - i\mathbf{q}\cdot\mathbf{v} + \frac{1}{\tau_{sz}^{\mathrm{DP}}}
\end{pmatrix}.
\tag{B3}
$$

The notation is defined in main text.

The extrinsic part of the diffusion matrix originates from two SOC sources, i.e., the one due to the external electric field and the other due to impurity potential. The contribution from the former one can be carried out from $(1/\tau)[\mathcal{I} - \langle(\mathcal{I} + \mathcal{K}_{\mathbf{k}})^{-1}(\mathcal{I} + \mathcal{T}_{\mathbf{k}})\rangle]_{\omega=0} - \mathcal{D}^{\mathrm{int}}$, leading to

$$
\mathcal{D}^{\mathrm{ext,E}} \simeq (1/\tau)\left[\langle \mathcal{K}_{\mathbf{k}} + \mathcal{K}_{\mathbf{k}}\mathcal{T}_{\mathbf{k}} - \mathcal{K}_{\mathbf{k}}^2 \rangle_{\omega=0} - \langle \mathcal{K}_{\mathbf{k}} + \mathcal{K}_{\mathbf{k}}\mathcal{T}_{\mathbf{k}} - \mathcal{K}_{\mathbf{k}}^2 \rangle_{\omega=0,\alpha'=0} \right]
$$

$$
= \begin{pmatrix}
0 & 0 & 0 & -i\left(\theta_{\mathrm{SH}}^{\mathrm{sj}}/2\right)(\mathbf{v}\times\mathbf{q})_z \\
-\left(\theta_{\mathrm{SH}}^{\mathrm{sj}}/2\right)v_y q_1 & 0 & i2\kappa(\mathbf{v}\times\mathbf{q})_z & \kappa v_x q_2 \\
-\left(\theta_{\mathrm{SH}}^{\mathrm{sj}}/2\right)v_x q_2 & -i2\kappa(\mathbf{v}\times\mathbf{q})_z & 0 & -\kappa v_y q_1 \\
-i\left(\theta_{\mathrm{SH}}^{\mathrm{sj}}/2\right)(\mathbf{v}\times\mathbf{q})_z & \kappa v_x q_2 & -\kappa v_y q_1 & 0
\end{pmatrix},
\tag{B4}
$$

where the spin-spin coupling is from $\langle -\mathcal{K}_{\mathbf{k}}^2 \rangle$. Similarly, we can calculate the contribution from the extrinsic SOC due to impurity potential. By substituting the three $\mathcal{M}$ matrices into $-\frac{1}{\tau}\langle(\mathcal{I} + \mathcal{K}_{\mathbf{k'}})^{-1}\mathcal{M}_{\mathbf{k'},\mathbf{k}}(\mathcal{I} + \mathcal{K}_{\mathbf{k}})^{-1}(\mathcal{I} + T_{\mathbf{k}})\rangle_{\omega=0}$, we obtain

$$
\mathcal{D}^{\mathrm{ext,sw}} \simeq (1/\tau)\langle \mathcal{K}_{\mathbf{k'}}\mathcal{M}_{\mathbf{k'},\mathbf{k}}^{\mathrm{sw}}\mathcal{T}_{\mathbf{k}} - \mathcal{K}_{\mathbf{k'}}\mathcal{M}_{\mathbf{k'},\mathbf{k}}^{\mathrm{sw}}\mathcal{K}_{\mathbf{k}} \rangle_{\omega=0}
$$

$$
= \begin{pmatrix}
0 & 0 & 0 & 0 \\
i\theta_{\mathrm{SH}}^{\mathrm{sj}} Dq_y q_1 & 0 & -i\kappa(\mathbf{v}\times\mathbf{q})_z & i\kappa Dq_x q_2 \\
i\theta_{\mathrm{SH}}^{\mathrm{sj}} Dq_x q_2 & i\kappa(\mathbf{v}\times\mathbf{q})_z & 0 & -i\kappa Dq_y q_1 \\
0 & -\kappa q_2(iDq_x + 2v_x) & \kappa q_1(iDq_y + 2v_y) & 2\kappa Dq_1 q_2
\end{pmatrix},
\tag{B5}
$$

$$
\mathcal{D}^{\mathrm{ext,inh}} \simeq (1/\tau)\langle \mathcal{K}_{\mathbf{k'}}\mathcal{M}_{\mathbf{k'},\mathbf{k}}^{\mathrm{inh}} - \mathcal{M}_{\mathbf{k'},\mathbf{k}}^{\mathrm{inh}}\mathcal{T}_{\mathbf{k}} + \mathcal{M}_{\mathbf{k'},\mathbf{k}}^{\mathrm{inh}}\mathcal{K}_{\mathbf{k}} \rangle_{\omega=0}
$$

$$
= \begin{pmatrix}
0 & -i\left(\theta_{\mathrm{SH}}^{\mathrm{sj}}/2\right)Dq_y q_1 & -i\left(\theta_{\mathrm{SH}}^{\mathrm{sj}}/2\right)Dq_x q_2 & -i\left(\theta_{\mathrm{SH}}^{\mathrm{sj}}/2\right)(\mathbf{v}\times\mathbf{q})_z \\
-i\left(\theta_{\mathrm{SH}}^{\mathrm{sj}}/2\right)Dq_y q_1 & 0 & 0 & 0 \\
-i\left(\theta_{\mathrm{SH}}^{\mathrm{sj}}/2\right)Dq_x q_2 & 0 & 0 & 0 \\
-i\left(\theta_{\mathrm{SH}}^{\mathrm{sj}}/2\right)(\mathbf{v}\times\mathbf{q})_z & 0 & 0 & 0
\end{pmatrix},
\tag{B6}
$$

$$
\mathcal{D}^{\mathrm{ext,ss}} \simeq -(1/\tau)\langle \mathcal{K}_{\mathbf{k'}}\mathcal{M}_{\mathbf{k'},\mathbf{k}}^{\mathrm{ss}}\mathcal{K}_{\mathbf{k}} \rangle_{\omega=0}
$$

$$
= \begin{pmatrix}
0 & -i\theta_{\mathrm{SH}}^{\mathrm{ss}} Dq_y q_1 & -i\theta_{\mathrm{SH}}^{\mathrm{ss}} Dq_x q_2 & -i\theta_{\mathrm{SH}}^{\mathrm{ss}}(\mathbf{v}\times\mathbf{q})_z \\
-\theta_{\mathrm{SH}}^{\mathrm{ss}}(v_y + iDq_y)q_1 & 0 & 0 & 0 \\
-\theta_{\mathrm{SH}}^{\mathrm{ss}}(v_x + iDq_x)q_2 & 0 & 0 & 0 \\
-i\theta_{\mathrm{SH}}^{\mathrm{ss}}(\mathbf{v}\times\mathbf{q})_z & 0 & 0 & 0
\end{pmatrix}.
\tag{B7}
$$

To calculate the contribution from the spin-precession scattering term, i.e., the last term in Eq. (37), we substitute $\tilde{g}_{\mathbf{k}}^i \simeq (1 + \tau e\mathbf{E} \cdot \nabla_{\mathbf{k}} - i\tau\mathbf{q} \cdot \mathbf{k}/m)g_k^i$ into $I^{(b)}$. After some straightforward calculation, we obtain the current from $\langle(\mathcal{K}_{\mathbf{k}} - \mathcal{I})I_{\mathbf{k}}^{(b)}\rangle$ and rewrite the result in the form of diffusion matrix as

$$\mathcal{D}^{\text{ext},(b)} = \begin{pmatrix} 0 & -i(\theta_{\text{SH}}^{\text{sj}}/2)Dq_y q_1 & -i(\theta_{\text{SH}}^{\text{sj}}/2)Dq_x q_2 & 0 \\ -(\theta_{\text{SH}}^{\text{sj}}/2)(3iDq_y + v_y)q_1 & 0 & 0 & 0 \\ -(\theta_{\text{SH}}^{\text{sj}}/2)(3iDq_x + v_x)q_2 & 0 & 0 & 0 \\ 0 & 0 & 0 & 0 \end{pmatrix}. \tag{B8}$$

Finally, we obtain the total extrinsic contribution in the diffusion matrix

$$\mathcal{D}^{\text{ext}} = \mathcal{D}^{\text{ext},E} + \mathcal{D}^{\text{ext,sw}} + \mathcal{D}^{\text{ext,inh}} + \mathcal{D}^{\text{ext,ss}} + \mathcal{D}^{\text{ext},(b)}. \tag{B9}$$

By collecting all the intrinsic and extrinsic pieces, we write out the final diffusion matrix shown in Eq. (38). Note that the extrinsic contribution is discarded in Eq. (38) for the matrix element containing intrinsic contribution, by taking into account the fact the extrinsic SOC is weaker than the intrinsic one.

APPENDIX C: DERIVATION OF THE DRIFT-DIFFUSION EQUATIONS FOR THE CURRENTS

The goal of this Appendix is to derive the transformation matrices $\hat{J}_x$ and $\hat{J}_y$, which connect the (spin) currents to the (spin) densities, so that one can obtain the currents directly from the densities via the equation

$$J_i^j(\mathbf{q}) = \hat{J}_i^{jl} S_{\mathbf{q}}^l. \tag{C1}$$

The transformation matrices, according to Eqs. (35) and (47), can be expressed as

$$\hat{J}_{x(y)}^{ij} = \langle\mathcal{J}_{x(y)\mathbf{k}}[\mathcal{I} + (\mathcal{I} + \mathcal{K}_{\mathbf{k}'})^{-1}\mathcal{M}_{\mathbf{k}',\mathbf{k}}](\mathcal{I} + \mathcal{K}_{\mathbf{k}})^{-1}(\mathcal{I} + T_{\mathbf{k}})\rangle_{ij} + (\tau/S_{\mathbf{q}}^j)\langle\mathcal{J}_{x(y)\mathbf{k}}[(\mathcal{I} + \mathcal{K}_{\mathbf{k}})^{-1}]^{il}I_{\mathbf{k}}^{(b),l}(\tilde{\mathbf{g}}_{j\mathbf{k}},\tilde{\mathbf{g}}_{j\mathbf{k}'})\rangle\big|_{\omega=0}, \tag{C2}$$

where the current matrices are given by

$$\mathcal{J}_{x(y)\mathbf{k}}^{ij} = (1/4)\text{Tr}[\sigma^i\{\sigma^j, \tilde{v}_{x(y)\mathbf{k}}\}]. \tag{C3}$$

Specifically, we have

$$\mathcal{J}_{x\mathbf{k}} = \begin{pmatrix} k_x/m & 0 & \lambda_1 & \alpha'\left(eE_y + \frac{k_y}{\tau}\right) \\ 0 & k_x/m & 0 & 0 \\ \lambda_1 & 0 & k_x/m & 0 \\ \alpha'\left(eE_y + \frac{k_y}{\tau}\right) & 0 & 0 & k_x/m \end{pmatrix} \tag{C4}$$

and

$$\mathcal{J}_{y\mathbf{k}} = \begin{pmatrix} k_y/m & \lambda_2 & 0 & -\alpha'\left(eE_x + \frac{k_x}{\tau}\right) \\ \lambda_2 & k_y/m & 0 & 0 \\ 0 & 0 & k_y/m & 0 \\ -\alpha'\left(eE_x + \frac{k_x}{\tau}\right) & 0 & 0 & k_y/m \end{pmatrix}, \tag{C5}$$

for the current flowing along the x and y directions, respectively. In the following, we take the current in the x direction as an example to show the details of perturbation calculation.

By using the same technique introduced in Appendix B, we obtain the intrinsic contribution

$$\hat{J}_x^{\text{int}} = \langle\mathcal{J}_x(\mathcal{I} + \mathcal{T} + \mathcal{K}^2 + \mathcal{K}^2\mathcal{T} - \mathcal{K} - \mathcal{K}\mathcal{T})\rangle_{\omega=0,\alpha'=0}$$

$$= \begin{pmatrix} -(iDq_x + v_x) & 0 & -\theta_{\text{SH}}^{\text{int}}Dq_2 & \theta_{\text{SH}}^{\text{int}}(iDq_y + v_y) \\ 0 & -(iDq_x + v_x) & 0 & Dq_1 \\ 0 & 0 & -(iDq_x + v_x) & 0 \\ \theta_{\text{SH}}^{\text{int}}(iDq_y + v_y) & -Dq_1 & 0 & -(iDq_x + v_x) \end{pmatrix}. \tag{C6}$$

With the same notation as used in the diffusion matrix, the relevant extrinsic terms are $\hat{J}_x^{\text{ext},E} = \langle\mathcal{J}_{x\mathbf{k}}(\mathcal{I} + \mathcal{T}_{\mathbf{k}} - \mathcal{K}_{\mathbf{k}})\rangle_{\omega=0} - \langle\mathcal{J}_{x\mathbf{k}}(\mathcal{I} + \mathcal{T}_{\mathbf{k}} - \mathcal{K}_{\mathbf{k}})\rangle_{\omega=0,\alpha'=0}$, $\hat{J}_x^{\text{ext,sw}} = \langle\mathcal{J}_{x\mathbf{k}'}\mathcal{M}_{\mathbf{k}',\mathbf{k}}^{\text{sw}}(\mathcal{T}_{\mathbf{k}} - \mathcal{K}_{\mathbf{k}})\rangle_{\omega=0}$, $\hat{J}_x^{\text{ext,inh}} = \langle\mathcal{J}_{x\mathbf{k}'}\mathcal{M}_{\mathbf{k}',\mathbf{k}}^{\text{inh}}\rangle$, and $\hat{J}_x^{\text{ext,ss}} = -\langle\mathcal{J}_{x\mathbf{k}'}\mathcal{M}_{\mathbf{k}',\mathbf{k}}\mathcal{K}_{\mathbf{k}}\rangle_{\omega=0}$,

resulting in

$$\hat{j}_x^{\text{ext,E}} = \begin{pmatrix} 0 & 0 & 0 & (\theta_{\text{SH}}^{\text{sj}}/2)v_y \\ 0 & 0 & -\kappa v_y & 0 \\ 0 & \kappa v_y & 0 & 0 \\ (\theta_{\text{SH}}^{\text{sj}}/2)v_y & 0 & 0 & 0 \end{pmatrix},$$ (C7)

$$\hat{j}_x^{\text{ext,sw}} = \begin{pmatrix} 0 & 0 & 0 & 0 \\ 0 & 0 & \kappa(iDq_y + v_y) & \kappa Dq_2 \\ \theta_{\text{SH}}^{\text{sj}}Dq_2 & -\kappa(iDq_y + v_y) & 0 & 0 \\ 0 & 0 & 0 & 0 \end{pmatrix},$$ (C8)

$$\hat{j}_x^{\text{ext,inh}} = \frac{\theta_{\text{SH}}^{\text{sj}}}{2} \begin{pmatrix} 0 & 0 & 0 & iDq_y \\ 0 & 0 & 0 & 0 \\ 0 & 0 & 0 & 0 \\ iDq_y & 0 & 0 & 0 \end{pmatrix},$$ (C9)

$$\hat{j}_x^{\text{ext,ss}} = \begin{pmatrix} 0 & 0 & -\theta_{\text{SH}}^{\text{ss}}Dq_2 & \theta_{\text{SH}}^{\text{ss}}(iDq_y + v_y) \\ 0 & 0 & 0 & 0 \\ 0 & 0 & 0 & 0 \\ \theta_{\text{SH}}^{\text{ss}}(iDq_y + v_y) & 0 & 0 & 0 \end{pmatrix}.$$ (C10)

The (spin) current induced by the spin-precession scattering term, at the leading order, can be directly calculated from $(J_x^{\text{ext},(b)})^j = \langle (k_x/m)\tau I^{(b),j} \rangle$ by substituting $\tilde{g}_{\mathbf{k}}^i \simeq g_k^i$. The result in the form of matrix leads to

$$\hat{j}_x^{\text{ext},(b)} = \theta_{\text{SH}}^{\text{sj}} \begin{pmatrix} 0 & 0 & -Dq_2 & 0 \\ 0 & 0 & 0 & 0 \\ -Dq_2 & 0 & 0 & 0 \\ 0 & 0 & 0 & 0 \end{pmatrix}.$$ (C11)

Then the extrinsic mechanisms totally contribute to the transformation matrices

$$\hat{j}_x^{\text{ext}} = \hat{j}_x^{\text{ext,E}} + \hat{j}_x^{\text{ext,sw}} + \hat{j}_x^{\text{ext,inh}} + \hat{j}_x^{\text{ext,ss}} + \hat{j}_x^{\text{ext},(b)}.$$ (C12)

Note that in the final result in Eqs. (48) and (49), only the leading term in each matrix element is retained.

APPENDIX D: DERIVATION OF SPIN-CURRENT SWAPPING

As mentioned in the main text, the spin current swapping in our theory is included as the second term in the collision integral $I_{\mathbf{k}}^{(0)}$, i.e., $-i\alpha'(2\pi\tau)^{-1}\int d\theta_{\mathbf{k}'}[\boldsymbol{\sigma}\cdot\mathbf{k}\times\mathbf{k}', \rho_{\mathbf{k}'}]$, and appears already in the first Born approximation. In the leading order, the correction in the steady-state density matrix due to spin current swapping term is given by

$$\delta g_{\mathbf{k}}^{\text{sw},j} = (2\alpha'/N_0)\sum_{lmn}\epsilon^{zlj}\epsilon^{zmn}k_m[J_n^l]^{(0)}, \quad (D1)$$

with the primary spin current $[J_n^l]^{(0)} = \sum_{\mathbf{k}'}k_n'g_{\mathbf{k}'}^l$. One then can calculate the swapped spin current from

$$\begin{aligned} [J_i^j]^{\text{SCS}} &\simeq \sum_{\mathbf{k}}(k_i/m)g_{\mathbf{k}}^{\text{sw},j} \\ &= \alpha'k_F^2\sum_{ln}\epsilon^{zlj}\epsilon^{zin}[J_n^l]^{(0)} \\ &= \alpha'k_F^2\left([J_j^i]^{(0)} - \delta_{ij}\sum_l[J_l^l]^{(0)}\right), \quad (D2) \end{aligned}$$

whose symmetry is consistent with previous work [29]. Here, the coefficient of spin-current swapping reads $\kappa = \alpha'k_F^2$.

[1] I. Žutić, J. Fabian, and S. Das Sarma, Rev. Mod. Phys. **76**, 323 (2004).

[2] J. Fabian, A. Matos-Abiague, C. Ertler, P. Stano, and I. Zutic, Acta Physica Slovaca **57**, 565 (2007).

[3] D. D. Awschalom and M. E. Flatté, Nat. Phys. **3**, 153 (2007).

[4] M. W. Wu, J. H. Jiang, and M. Q. Weng, Phys. Rep. **493**, 61 (2010).

[5] M. I. D'yakonov and V. I. Perel', JETP Lett. **13**, 467 (1971).

[6] S. Murakami, N. Nagaosa, and S.-C. Zhang, Science **301**, 1348 (2003).

[7] J. Sinova, D. Culcer, Q. Niu, N. A. Sinitsyn, T. Jungwirth, and A. H. MacDonald, Phys. Rev. Lett. **92**, 126603 (2004).

[8] Y. K. Kato, R. C. Myers, A. C. Gossard, and D. D. Awschalom, Science **306**, 1910 (2004).

[9] J. Wunderlich, B. Kaestner, J. Sinova, and T. Jungwirth, Phys. Rev. Lett. **94**, 047204 (2005).

[10] E. L. Ivchenko and G. E. Pikus, JETP Lett. **27**, 604 (1978).

[11] V. M. Edelstein, Solid State Commun. **73**, 233 (1990).

[12] L. S. Levitov, Y. V. Nazarov, and G. M. Éliashberg, Sov. Phys. JETP **61**, 133 (1985).

[13] A. G. Aronov and Y. B. Lyanda-Geller, JETP Lett. **50**, 431 (1989).

[14] Y. K. Kato, R. C. Myers, A. C. Gossard, and D. D. Awschalom, Phys. Rev. Lett. **93**, 176601 (2004).

[15] A. Y. Silov, P. A. Blajnov, J. H. Wolter, R. Hey, K. H. Ploog, and N. S. Averkiev, Appl. Phys. Lett. **85**, 5929 (2004).

[16] V. Sih, R. C. Myers, Y. K. Kato, W. H. Lau, A. C. Gossard, and D. D. Awschalom, Nat. Phys. **1**, 31 (2005).

[17] R. H. Silsbee, J. Phys.: Condens. Matter **16**, R179 (2004).

[18] E. Saitoh, M. Ueda, H. Miyajima, and G. Tatara, Appl. Phys. Lett. **88**, 182509 (2006).

[19] K. Ando and E. Saitoh, Nat. Commun. **3**, 629 (2012).

[20] J. C. R. Sánchez, L. Vila, G. Desfonds, S. Gambarelli, J. P. Attané, J. M. D. Teresa, C. Magén, and A. Fert, Nat. Commun. **4**, 2944 (2013).

[21] S. D. Ganichev, E. L. Ivchenko, V. V. Belkov, S. A. Tarasenko, M. Sollinger, D. Weiss, W. Wegscheider, and W. Prettl, Nature (London) **417**, 153 (2002).

[22] E. L. Ivchenko, Y. B. Lyanda-Geller, and G. E. Pikus, JETP Lett. **50**, 175 (1989).

[23] E. L. Ivchenko, Y. B. Lyanda-Geller, and G. E. Pikus, Sov. Phys. JETP **71**, 550 (1990).

[24] V. Sih, W. H. Lau, R. C. Myers, V. R. Horowitz, A. C. Gossard, and D. D. Awschalom, Phys. Rev. Lett. **97**, 096605 (2006).

[25] K. Ando, J. Ieda, S. Sasage, S. Takahashi, S. Maekawa, and E. Saitoh, Appl. Phys. Lett. **94**, 262505 (2009).

[26] Y. Kajiwara, K. Harii, S. Takahashi, J. Ohe, K. Uchida, M. Mizuguchi, H. Umezawa, H. Kawai, K. Ando, K. Takanashi, S. Maekawa, and E. Saitoh, Nature (London) **464**, 262 (2010).

[27] L. Liu, C.-F. Pai, Y. Li, H. W. Tseng, D. C. Ralph, and R. A. Buhrman, Science **336**, 555 (2012).

[28] L. Liu, O. J. Lee, T. J. Gudmundsen, D. C. Ralph, and R. A. Buhrman, Phys. Rev. Lett. **109**, 096602 (2012).

[29] M. B. Lifshits and M. I. Dyakonov, Phys. Rev. Lett. **103**, 186601 (2009).

[30] S. Sadjina, A. Brataas, and A. G. Mal'shukov, Phys. Rev. B **85**, 115306 (2012).

[31] A. R. Cameron, P. Riblet, and A. Miller, Phys. Rev. Lett. **76**, 4793 (1996).

[32] C. P. Weber, N. Gedik, J. E. Moore, J. Orenstein, J. Stephens, and D. D. Awschalom, Nature (London) **437**, 1330 (2005).

[33] L. Yang, J. D. Koralek, J. Orenstein, D. R. Tibbetts, J. L. Reno, and M. P. Lilly, Phys. Rev. Lett. **106**, 247401 (2011).

[34] M. P. Walser, C. Reichl, W. Wegscheider, and G. Salis, Nat. Phys. **8**, 757 (2012).

[35] B. Anderson, T. D. Stanescu, and V. Galitski, Phys. Rev. B **81**, 121304 (2010).

[36] K. Shen and G. Vignale, Phys. Rev. Lett. **111**, 136602 (2013).

[37] A. Ferreira, T. G. Rappoport, M. A. Cazalilla, and A. H. Castro Neto, Phys. Rev. Lett. **112**, 066601 (2014).

[38] J. Balakrishnan, G. K. W. Koon, A. Avsar, Y. Ho, J. H. Lee, M. Jaiswal, S.-J. Baeck, J.-H. Ahn, A. Ferreira, M. A. Cazalilla, A. H. C. Neto, and B. Özyilmaz, Nat. Commun. **5**, 4748 (2014).

[39] R. Raimondi and P. Schwab, Physica E **42**, 952 (2010).

[40] C. Gorini, P. Schwab, R. Raimondi, and A. L. Shelankov, Phys. Rev. B **82**, 195316 (2010).

[41] P. Schwab, R. Raimondi, and C. Gorini, Europhys. Lett. **90**, 67004 (2010).

[42] R. Raimondi, P. Schwab, C. Gorini, and G. Vignale, Ann. Phys. **524**, 153 (2012).

[43] R. J. Elliott, Phys. Rev. **96**, 266 (1954).

[44] Y. Yafet, *Solid State Physics* (Academic, New York, 1963), Vol. 14.

[45] M. I. D'yakonov and V. I. Perel', Zh. Eksp. Teor. Fiz. **60**, 1954 (1971) [Sov. Phys. JETP **33**, 1053 (1971)].

[46] K. Shen, G. Vignale, and R. Raimondi, Phys. Rev. Lett. **112**, 096601 (2014).

[47] L. Yang, J. D. Koralek, J. Orenstein, D. R. Tibbetts, J. L. Reno, and M. P. Lilly, Nat. Phys. **8**, 153 (2012).

[48] A. A. Burkov, A. S. Núñez, and A. H. MacDonald, Phys. Rev. B **70**, 155308 (2004).

[49] E. G. Mishchenko, A. V. Shytov, and B. I. Halperin, Phys. Rev. Lett. **93**, 226602 (2004).

[50] P. Kleinert and V. V. Bryksin, Phys. Rev. B **76**, 205326 (2007).

[51] V. V. Bryksin and P. Kleinert, Phys. Rev. B **75**, 205317 (2007).

[52] X. Liu and J. Sinova, Phys. Rev. B **86**, 174301 (2012).

[53] E. M. Hankiewicz and G. Vignale, Phys. Rev. Lett. **100**, 026602 (2008).

[54] Y. A. Bychkov and E. I. Rashba, J. Phys. C **17**, 6039 (1984).

[55] G. Dresselhaus, Phys. Rev. **100**, 580 (1955).

[56] J. Rammer, *Quantum Field Theory of Nonequilibrium States* (Cambridge University Press, Cambridge, 2007).

[57] H. Haug and A.-P. Jauho, *Quantum Kinetics in Transport and Optics of Semiconductors*, Springer Series in Solid-State Sciences Vol. 123 (Springer, Berlin, 1996).

[58] K. Shen, G. Tatara, and M. W. Wu, Phys. Rev. B **83**, 085203 (2011).

[59] P. Lipavský, V. Špička, and B. Velický, Phys. Rev. B **34**, 6933 (1986).

[60] D. Culcer, E. M. Hankiewicz, G. Vignale, and R. Winkler, Phys. Rev. B **81**, 125332 (2010).

[61] X. Bi, P. He, E. M. Hankiewicz, R. Winkler, G. Vignale, and D. Culcer, Phys. Rev. B **88**, 035316 (2013).

[62] J. L. Cheng and M. W. Wu, J. Phys.: Condens. Matter **20**, 085209 (2008).

[63] H.-A. Engel, B. I. Halperin, and E. I. Rashba, Phys. Rev. Lett. **95**, 166605 (2005).

[64] W.-K. Tse and S. Das Sarma, Phys. Rev. Lett. **96**, 056601 (2006).

[65] N. S. Averkiev and L. E. Golub, Semicond. Sci. Technol. **23**, 114002 (2008).

[66] J. H. Jiang, Y. Zhou, T. Korn, C. Schüller, and M. W. Wu, Phys. Rev. B **79**, 155201 (2009).

[67] R. Raimondi, C. Gorini, P. Schwab, and M. Dzierzawa, Phys. Rev. B **74**, 035340 (2006).

[68] E. M. Hankiewicz and G. Vignale, Phys. Rev. B **73**, 115339 (2006).

[69] E. M. Hankiewicz, G. Vignale, and M. E. Flatté, Phys. Rev. Lett. **97**, 266601 (2006).

[70] K. Uchida, S. Takahashi, K. Harii, J. Ieda, W. Koshibae, K. Ando, S. Maekawa, and E. Saitoh, Nature (London) **455**, 778 (2008).

[71] X. Lou, C. Adelmann, S. A. Crooker, E. S. Garlid, J. Zhang, K. S. M. Reddy, S. D. Flexner, C. J. Palmstrom, and P. A. Crowell, Nat. Phys. **3**, 197 (2007).

[72] K. Shen and G. Vignale, Phys. Rev. Lett. **110**, 096601 (2013).

[73] J. M. Kikkawa and D. D. Awschalom, Nature (London) **397**, 139 (1999).

[74] M. E. Flatté and J. M. Byers, Phys. Rev. Lett. **84**, 4220 (2000).

[75] I. D'Amico and G. Vignale, Phys. Rev. B **62**, 4853 (2000).

[76] K. Flensberg, T. S. Jensen, and N. A. Mortensen, Phys. Rev. B **64**, 245308 (2001).

[77] B. A. Bernevig, J. Orenstein, and S.-C. Zhang, Phys. Rev. Lett. **97**, 236601 (2006).

[78] C. P. Weber, J. Orenstein, B. A. Bernevig, S.-C. Zhang, J. Stephens, and D. D. Awschalom, Phys. Rev. Lett. **98**, 076604 (2007).

[79] M. Q. Weng, M. W. Wu, and H. L. Cui, J. Appl. Phys. **103**, 063714 (2008).

[80] J. D. Koralek, C. P. Weber, J. Orenstein, B. A. Bernevig, S. C. Zhang, S. Mack, and D. D. Awschalom, Nature (London) **458**, 610 (2009).

[81] V. A. Slipko, I. Savran, and Y. V. Pershin, Phys. Rev. B **83**, 193302 (2011).

[82] I. V. Tokatly and E. Y. Sherman, Phys. Rev. A **87**, 041602 (2013).

[83] L. Yang, J. Orenstein, and D.-H. Lee, Phys. Rev. B **82**, 155324 (2010).

[84] M. Q. Weng and M. W. Wu, Phys. Rev. B **86**, 205307 (2012).

[85] J. Wanner, C. Gorini, P. Schwab, and U. Eckern, Adv. Mater. Interfaces **1**, 1400181 (2014).